



HAL
open science

Early Carboniferous lignophyte tree diversity in Australia: Woods from the Drummond and Yarrol basins, Queensland

Anne-Laure Decombeix, Jean Galtier, Stephen Mcloughlin, Brigitte Meyer-Berthaud, Gregory Webb, Paul Blake

► **To cite this version:**

Anne-Laure Decombeix, Jean Galtier, Stephen Mcloughlin, Brigitte Meyer-Berthaud, Gregory Webb, et al.. Early Carboniferous lignophyte tree diversity in Australia: Woods from the Drummond and Yarrol basins, Queensland. *Review of Palaeobotany and Palynology*, 2019, 263, pp.47-64. 10.1016/j.revpalbo.2019.01.009 . hal-02132903

HAL Id: hal-02132903

<https://hal.science/hal-02132903>

Submitted on 12 Oct 2021

HAL is a multi-disciplinary open access archive for the deposit and dissemination of scientific research documents, whether they are published or not. The documents may come from teaching and research institutions in France or abroad, or from public or private research centers.

L'archive ouverte pluridisciplinaire **HAL**, est destinée au dépôt et à la diffusion de documents scientifiques de niveau recherche, publiés ou non, émanant des établissements d'enseignement et de recherche français ou étrangers, des laboratoires publics ou privés.

1 **Early Carboniferous lignophyte tree diversity in Australia: woods**
2 **from the Drummond and Yarrol basins, Queensland.**

3

4 Anne-Laure Decombeix^{1,2,*}, Jean Galtier¹, Stephen McLoughlin³, Brigitte Meyer-Berthaud¹,
5 Gregory E. Webb⁴, Paul R. Blake⁵.

6

7 *¹AMAP, Univ Montpellier, CNRS, CIRAD, INRA, IRD, Montpellier, France*

8 *²Department of Ecology and Evolutionary Biology, and Natural History Museum and*
9 *Biodiversity Institute, University of Kansas, Lawrence, KS 66045-7534, USA*

10 *³Department of Palaeobiology, Swedish Museum of Natural History, Box 50007, S-104 05*
11 *Stockholm, Sweden*

12 *⁴School of Earth and Environmental Sciences, The University of Queensland, Brisbane QLD*
13 *4072, Australia*

14 *⁵Geological Survey of Queensland, Department of Natural Resources, Mines & Energy, PO*
15 *Box 15216, City East, Queensland 4002, Australia.*

16

17 * Corresponding author, e-mail: anne-laure.decombeix@cirad.fr

19 **Abstract:** Early Carboniferous (Mississippian) permineralised woods from Australia with
20 multiseriate rays have been customarily assigned or compared to the European genus *Pitus*,
21 despite the absence of information on their primary vascular anatomy. In the context of
22 continuing work on the diversity of Late Devonian and Mississippian floras of Gondwana, we
23 studied new silicified woods with secondary xylem similar to that of *Pitus* (multiseriate rays,
24 araucarioid radial pitting) from two sedimentary basins of Queensland, Australia. In the
25 Drummond Basin, three morphotypes of wood of Viséan age can be distinguished based on
26 ray size in tangential section. Although this variation is similar to that observed between the
27 various European species of *Pitus*, information on the primary vascular anatomy of the trees
28 provided by three incomplete specimens excludes an affinity with *Pitus* for at least two taxa.
29 In the Yarrol Basin, two well-preserved late Viséan trunks also have characters similar to
30 *Pitus* but can be distinguished from that genus and other previously described Mississippian
31 trees, in particular by the anatomy of their primary vascular system and departing leaf traces.
32 They are assigned to a new genus, *Ninsaria*. Collectively, the new specimens from
33 Queensland show that wood traditionally referred to ‘*Pitus*’ from Australia actually belongs to
34 several other types of trees that are not known from Europe or North America, indicating
35 probable floristic provincialism between the Northern and Southern hemisphere floras at this
36 time. These new fossils corroborate the existence of a global Mississippian diversification of
37 (pro)gymnosperm trees already noted in Laurussia. They also indicate that the Mississippian
38 floras of Australia were more diverse and complex than traditionally inferred.

39

40 **Key-words:** Fossil wood; progymnosperms; gymnosperms; Tournaisian; Viséan; eastern
41 Australia

43 1. Introduction

44 This study is part of a continuing investigation of the Late Devonian and Early
45 Carboniferous (Mississippian) floristic diversity of Gondwana, and comparison to floras of
46 Laurussia. A significant diversification of ferns s.l. and lignophytes (progymnosperms and
47 seed plants) during the Mississippian is suggested by anatomically preserved axes from
48 Europe and North America (e.g., Galtier and Scott, 1985; Galtier, 1988; Dunn, 2006; Galtier
49 and Meyer-Berthaud, 2006; Taylor et al., 2009). However, their pattern of diversification in
50 other regions of the world remains obscure owing to the paucity of well-documented
51 specimens from this period. For the supercontinent Gondwana, the most recent general
52 synthesis (Anderson et al., 1999) suggested a significant delay in diversification of seed plants
53 and ferns compared to the northern continents. However, recent studies suggest that these
54 plant groups were present in Gondwana earlier than inferred, at least in the palaeotropics (see
55 Prestianni et al., 2015 for a discussion of high-latitude floras). Australia constitutes a key-
56 region in these investigations, with a significant number of Mississippian anatomically
57 preserved ferns and lignophytes discovered recently at localities in the northeastern part of the
58 country (Hueber and Galtier, 2002; Galtier et al., 2007; Decombeix et al., 2011b).

59 The presence of carbonised or permineralised gymnospermous wood of Mississippian age
60 in Australia has been reported since at least the 19th century (e.g., Jack and Etheridge, 1892;
61 Chapman, 1904; Walkom, 1928; Cook and Rozefelds, 2015). Most reported specimens occur
62 in Viséan (Middle Mississippian) formations and have been assigned to *Pitus*, a genus
63 represented in Europe by large trunks as much as 2 m in diameter and interpreted to have seed
64 plant affinities (e.g., Long, 1979; Galtier, 2002). However, the anatomy of the primary
65 vascular system of the Australian stems has not been described to date, and their assignment
66 to *Pitus* is based solely on the occurrence of multiseriate rays in the secondary xylem. Using
67 this character, Walkom (1928) erected the new species *Pitys* (= *Pitus*) *sussmilchii* for

68 permineralised woods found in coarse-grained sedimentary rocks of the ‘Kuttung Series’
69 (now Kuttung Formation; Mond, 1973) near Wallaroba, New South Wales (southeastern
70 Australia). This decision was later criticised by Gordon (1935), who emphasised that the
71 anatomical information available in Walkom's specimen was not sufficient to assign it to
72 *Pitus*. Other woods subsequently documented at Viséan localities of New South Wales have,
73 nevertheless, been assigned to *Pitus* sp. (e.g., Gould, 1975; McKelvey and McPhie, 1985;
74 Morris, 1985). In Queensland (northeastern Australia), Mississippian permineralised woods,
75 including complete trunks, also have been reported but without detailed descriptions or study
76 of their affinities. Following two collecting trips in 2005 and 2008, the presence of three
77 morphotaxa of lignophyte trees was documented in Lower Mississippian deposits of the
78 Broken River Province and the Burdekin Basin, in northeastern Queensland (Fig. 1;
79 Decombeix et al., 2011b). Two of these Tournaisian taxa have a wood anatomy very distinct
80 from *Pitus*. They were assigned to the new genus *Dameria* and to *Protopitys*, a putative
81 heterosporous progymnosperm also known from the Mississippian of Europe and North
82 America (Walton, 1957; Galtier and Scott, 1990; Galtier et al., 1998; Falcon-Lang and
83 Galtier, 2010; Decombeix et al., 2015). The third taxon has a wood anatomy similar to that of
84 *Pitus*, with multiseriate rays and araucarioid radial and cross-field pitting. However, it differs
85 significantly in its pattern of leaf trace emission and in its bark anatomy (Decombeix et al.,
86 2011b; Decombeix, 2013) and should be assigned to a new taxon when enough anatomical
87 information is gathered to characterize it.

88 Here, we describe slightly younger permineralised wood specimens collected in Middle
89 Mississippian (Viséan) deposits of two other basins of eastern Queensland (Fig. 1). These
90 specimens also have secondary xylem anatomy broadly similar to *Pitus*. From the Drummond
91 Basin, three wood morphotypes can be recognised based on ray size in tangential section, a
92 variation similar to that observed between European species of *Pitus*. In the Yarrol Basin, two

93 trunk fragments with *Pitus*-like anatomy were collected. We show, based on leaf traces, pith
94 and primary xylem anatomy, that these woods differ from *Pitus*, and from all other
95 contemporaneous taxa. We discuss their implications for understanding Mississippian floristic
96 diversity in Australia.

97

98 **2. Material and methods**

99 ***2.1. Drummond Basin woods***

100 The Upper Devonian to Mississippian Drummond Basin in central Queensland contains
101 predominantly terrestrial sedimentary and volcanic rocks (Veevers et al., 1964; Olgers, 1972,
102 Blake et al., 2012, Purdy et al., 2016), deposited in an extensional foreland basin located on
103 the western margin of the New England Orogen (Fig. 1; Johnson and Henderson, 1991; Davis
104 and Henderson, 1996; Henderson et al., 1998). Three depositional cycles can be recognised
105 (Fig. 2). Cycle 1 (Upper Devonian to Mississippian) corresponds to a continental succession
106 deposited close to a volcanic terrane and is essentially composed of lavas, pyroclastic deposits
107 and richly volcanoclastic sedimentary rocks and sinter deposits, locally hosting permineralised
108 plants (Walter et al., 1996, 1998). Cycle 2 (Mississippian) is represented chiefly by fluvial
109 sandstones. Cycle 3 (Mississippian) is again dominated by felsic–intermediate volcanics and
110 volcanogenic sedimentary rocks. The fossil woods described in this paper were collected from
111 the Ducabrook Formation, within cycle 3. The Ducabrook Formation is more than 2 km thick
112 and has been interpreted to represent fluvial and lacustrine deposits (Olgers, 1972), although
113 shallow-marine incursions may have occurred locally (Veevers et al., 1964). The formation is
114 famous for its middle to late Viséan freshwater fauna that includes the remains of sharks,
115 acanthodians, rhizodonts, lungfishes, and the oldest tetrapod body fossil known thus far in
116 Gondwana (e.g., Thulborn et al., 1996; Warren and Turner, 2004). The similarity of this
117 assemblage to contemporaneous vertebrate assemblages from the Euramerican zone

118 (Thulborn et al., 1996) supports the idea of a continental connection between Laurussia and
119 Gondwana during the Late Devonian and/or Mississippian.

120 Plant megafossils from the Ducabrook Formation include *Lepidodendron* and *Stigmaria*
121 (Veevers et al., 1964; White, 1964, 1969, 1986), zygopterid fern stems (S. McLoughlin,
122 unpub. data), and woody axes. This paper focuses on eleven wood specimens collected by the
123 Geological Survey of Queensland at a locality about 120 km southwest of Clermont, in the
124 southern Drummond Basin (coordinates 23°51'36"S, 147°2'24"E; Fig. 2) where fossil wood is
125 relatively common. Palynological studies have indicated a middle to late Viséan age for the
126 Ducabrook Formation (Playford, 1978, 1985; Jones, 1996; Jones et al., 2000). However,
127 palynological sampling for these studies was undertaken relatively high in the >2-km-thick
128 Ducabrook Formation. Both the conformably underlying Star of Hope Formation and the
129 Ducabrook Formation are currently interpreted to be Viséan (Jell, 2013). The wood specimens
130 were collected near the base of the formation whereas other studies were carried out near its
131 top, but the exact age of the base of the Ducabrook Formation is very poorly constrained and
132 we thus favour a general Viséan age for the new specimens. The wood fragments, with field
133 numbers DBW1–DBW11, are strongly silicified and have been studied using classical thin-
134 sections and wafers (Hass and Rowe, 1999) prepared at the University of Queensland (and
135 stored in the collections of the Queensland Museum), and at UMR AMAP, Montpellier.

136

137 **2.2. Yarrol Basin trunks**

138 The Yarrol Basin is a forearc basin formed during the Middle Devonian to early Permian
139 (Cisuralian) on the eastern side of the New England Fold Belt (orogen), which developed
140 along the active convergent margin of eastern Australia at that time (Figs 1, 3). It contains a
141 thick succession of almost exclusively marine deposits (Murray et al., 1987). The lithological
142 succession has been influenced strongly by contemporaneous felsic–intermediate volcanic

143 activity of varying intensity on the adjacent orogen (Maxwell, 1964). The thick succession of
144 Mississippian marine clastic–volcaniclastic sediments contains sporadic carbonate units,
145 including several coral-sponge-microbial reefs (Simpson et al., 2012).

146 Two portions of decorticated trunks (field numbers YB1 and YB2) were collected in the
147 northern part of the Yarrol Basin (23°22'45"S, 150°15'24"E) from an un-named unit in the
148 Rockhampton Group in the original group type area (Fleming, 1967). The trunks occurred in
149 poorly exposed calcareous siltstone and sandstone containing corals and bryozoans between
150 the Lion Creek Limestone and a higher, unnamed limestone that is now known to contain
151 coral faunule D corals equivalent to limestone FC5 of Webb (1990) rather than faunule C
152 corals of the Lion Creek Limestone. The higher limestone was originally considered part of
153 the Lion Creek Limestone faulted into its current position (Webb, 1990), but it is now
154 considered a younger limestone beneath the Pennsylvanian–Cisuralian Lorrain Formation (as
155 defined by Murray et al., 2012) (Fig. 3). The Rockhampton Group is Mississippian, and the
156 age of the unit yielding the wood specimens is constrained to the late Viséan based on coral
157 and brachiopod biostratigraphy (i.e., between coral faunules C and D of Webb, 1990) placing
158 it near the boundaries of the *Rhipidomella fortimuscula* and *Marginirugus barringtonensis*
159 brachiopod zones (Roberts et al., 1993) and the *Montognathus carinatus* and *Gnathodus*
160 *texanus* – *Gn. bilineatus* conodont zones (Jenkins et al., 1993; Denayer and Webb, 2015).
161 YB1 was cut into 13 pieces labelled A to M at the University of Queensland and thin-sections
162 were prepared from all portions. YB2 is 14.5 × 9 cm in diameter and allows observation of a
163 whole trunk in cross-section. New thin-sections (Hass and Rowe, 1999) and acetate peels
164 using HF (Galtier and Phillips, 1999) were also prepared at UMR AMAP, Montpellier on
165 both YB1 A-M and YB2 to provide additional information.

166

167 **2.3. Methods**

168 Images were taken using Sony XCD-U100CR digital cameras attached to an Olympus SZX12
169 stereomicroscope and to an Olympus BX51 compound microscope. Cropping, rotation, and
170 adjustments of brightness and contrast of the digital images were applied using Photoshop
171 CS5 version 12.0 (Adobe Systems Inc). Cell and tissue dimensions were measured using
172 ImageJ version 1.45 (Rasband, 1997–2016).

173 All specimens and slides are part of the collections of the Queensland Museum. Field
174 numbers DBW- and YB- are used in this paper; museum registration numbers and fossil
175 locality details are available upon request to the Geosciences Department of the Queensland
176 Museum, Brisbane.

177

178 **3. Woods from the Drummond Basin**

179 *3.1. Descriptions (Plates I–III)*

180 All the specimens possess gymnospermous secondary xylem composed of tracheids and
181 multiseriate parenchymatous rays (Plate I). Specimens DBW1–DBW3, DBW5, DBW7–
182 DBW8, DBW10 and DBW11 represent pieces of wood with no primary tissues preserved.
183 DBW6 is a piece of wood containing vascular traces to lateral appendages. DBW4
184 corresponds to the central part of an axis with a very compressed and poorly preserved stele
185 surrounded by several centimetres of secondary xylem. DBW9 is also the central part of an
186 axis but, in this case, with the pith and innermost secondary xylem preserved.

187 In the following description, we first document the wood anatomy for all specimens, then
188 focus on those providing additional information (DBW4, 6, and 9).

189

190 *3.1.1. Wood anatomy (all specimens) (Plate I; Fig. 4; Table 1)*

191 With the exception of DBW4, DBW6 and DBW9, which represent the central portions of
192 axes, all specimens correspond to fragments of wood 2–5 cm wide that incorporate parallel
193 files of tracheids and are thus interpreted as representing the outer parts of large axes.

194 In cross-section, the tracheids are rectangular, more rarely polygonal, with an average
195 diameter of 40–50 μm between the specimens (maximum observed diameter 75 μm). All
196 specimens incorporate changes in tracheid radial diameter that form more or less obvious
197 growth rings (Plate I, 1, 4, 7). The preservation of the specimens does not, however, permit
198 accurate measurement of the thickness of those rings, because some portions are considerably
199 distorted. The best preserved examples are a few millimetres thick (e.g., 4 and 7 mm in
200 DBW2). The multiseriate rays are long in transverse section, and separate 4–10 rows of
201 tracheids (Plate I, 1, 4, 7) depending on the specimen and location within a single specimen.

202 In radial longitudinal section, the tracheid walls have 1–4, commonly two, rows of
203 araucarioid pits that are 6–11 μm in diameter (Plate I, 3, 6, 9). The pit aperture is oval and
204 oblique. In some sections, the pits cover the entire width of the radial wall (e.g., Plate I, 6),
205 whereas in others they are more spaced (e.g., Plate I, 3, 9). In those specimens where cross-
206 field pitting is preserved, it is typically araucarioid, with numerous small crowded pits (arrows
207 on Plate I, 3, 9). Ray cells are radially elongate, with vertical to oblique end walls, and many
208 have dark contents.

209 Although the type of radial pitting is similar in all the specimens, it is possible to
210 distinguish three morphotypes based on ray size in tangential sections (Plate I, 2, 5, 8). A
211 summary of the ray characteristics is given for the best preserved specimens of each type
212 (Table 1) and their general aspect is illustrated (Fig. 4). All types show evidence of ray fusion
213 in tangential longitudinal section.

214 The first morphotype is represented by a single specimen, DBW2. It is characterised by
215 rays that are 1–3 cells wide (mean: 1.8) and 1–20 (mean: 6.2) cells high in tangential

216 longitudinal section (Plate I, 2). Ray cells are circular to rectangular in tangential section and
217 have an average size of $22 \times 31 \mu\text{m}$. Ray density is 9 rays/ mm^2 .

218 The second morphotype is the most abundant, represented by specimens DBW3, DBW4,
219 DBW6, DBW7, DBW10 and DBW11. Specimen DBW6, in which the best preservation of
220 wood characters is found, is used to characterise that morphotype. Rays are 1–4 cells wide
221 (mean 2.4) and 1–60 cells high (mean: 21.7) (Plate I, 5). Individual ray cells tend to be
222 rectangular in tangential section and have an average size relatively similar to the previous
223 type, $18 \times 31 \mu\text{m}$. Ray density is lower, at 5 rays/ mm^2 .

224 Finally, the third morphotype, represented by DBW5 and DBW8, is characterised by rays
225 that are 1–8 cells wide (mean 4.5) and 1–25 cells high (mean 11) (Plate I, 8). Ray cells in
226 these specimens are much more circular in tangential section than in the two previous forms,
227 and have average dimensions of $27 \times 29 \mu\text{m}$. Ray density is 6.5/ mm^2 .

228

229 *3.1.2. Compressed axis (DBW4) (Plate II, 1-4; Fig. 5)*

230 This specimen is an axis $5.3 \times 4.4 \text{ cm}$ in diameter. The central zone, which corresponds to
231 the pith and primary xylem, is $1.2 \times 0.3 \text{ cm}$ in cross-section; the oblong shape is probably due
232 to strong compression of the axis (Fig. 5). Cells of the central zone have been replaced by
233 crystals, so the anatomy of the pith and primary xylem remains unknown. However, several
234 small vascular strands and traces to lateral appendages are evident at the periphery of this
235 region (Fig. 5; Plate II, 1–4). Maturation appears to be endarch in most of the strands and in
236 some of the traces as they depart from the stele (Plate II, 1). Further away, the traces have a
237 more mesarch aspect with a small amount of parenchyma on their adaxial side (Plate II, 2).
238 The departing traces are small (slightly less than $300 \mu\text{m}$ in diameter). The primary xylem
239 tracheids of the traces are up to $60 \mu\text{m}$ in diameter. Up to nine of these vascular traces are
240 evident on a single transverse section, indicating a compact organotaxis in this part of the

241 axis, and traces can be followed on successive sections 2 mm apart (Fig. 5). Their
242 arrangement (Fig. 5A), suggests that they may have been produced in groups of three.
243 However, the order of emission of the traces within each group is not obvious. No traces were
244 observed further than 3 mm from the pith, which suggests that the vascularised organs were
245 abscised early in the ontogeny of the axis.

246 The secondary xylem of the specimen is compressed and it is difficult to assess the
247 presence of growth interruptions. Where they are well-preserved, the secondary xylem
248 tracheids are square to rectangular in transverse section. Their radial walls have 1–3 rows of
249 araucarioid pits with a small aperture. Rays are uni- to triseriate and high in tangential
250 longitudinal section and correspond to those of the second wood morphotype described above.

251

252 *3.1.3. Wood with vascular traces to lateral appendages (DBW6) (Plate II, 5–6)*

253 DBW6 is a piece of secondary xylem in which tracheid files tend to be strongly convergent
254 indicating that the centre of the axis was very close to the preserved portion. In its most
255 internal part, the wood contains a group of three small successive vascular traces that are very
256 close to each other (Plate II, 5). Each trace contains a single strand of protoxylem and is
257 accompanied by a very small amount of parenchyma on its abaxial side (Plate II, 6). The
258 wood is of the same type (second morphotype) as the preceding specimen.

259

260 *3.1.4. Central part of axis (DBW9) (Plate III)*

261 This small specimen is 2.5 cm in diameter and corresponds to a piece of parenchymatous
262 pith with a small portion of secondary wood preserved on one side (Plate III, 1). In addition to
263 typical parenchyma cells, the pith also contains isodiametric cells with thicker walls that form
264 0.5–1-mm-wide dark clusters (Plate III, 1–3). Because only the innermost part of the wood
265 (<2 mm) is preserved, ray size is difficult to interpret but rays appear to be uni- to biseriate

266 and similar to the first or second wood morphotype (Plate III, 4). Limited information on the
267 primary xylem and on a departing leaf trace is available from the small zone preserving the
268 pith–secondary xylem boundary (Plate III, 1, 4, 5). All primary xylem strands appear to be in
269 contact with the secondary xylem, i.e., no medullary or peri-medullary strands are evident
270 (Plate III, 1, 4). The departing trace contains a single mesarch strand of primary xylem (Plate
271 III, 5) and a small strand (not visible on the photo) appears to be lying in a radial to slightly
272 oblique plane from the trace. Because the preservation of the pith–secondary xylem boundary
273 is not only restricted to a small sector of the specimen but also to a very short vertical
274 distance, the whole process of trace emission could not be investigated further.

275

276 *3.2 Affinities*

277 The new specimens from the Drummond Basin raise two main questions: (1) how many taxa
278 are present? and (2) how do they compare to *Pitus*, the genus to which similar woods have
279 traditionally been assigned in Australia? We will first discuss how the different morphotypes
280 of wood found in the Ducabrook Formation answer these questions, then we will show the
281 significant insights revealed by the specimens with a partly preserved primary vascular
282 system.

283

284 *3.2.1. Do the different wood morphotypes represent different taxa?*

285 When the average ray width and height of the three specimens representing the types are
286 compared, T-test (95%) results indicate that DBW6 has significantly higher rays than DBW2
287 and DBW5, and DBW5 has significantly broader rays than the two other specimens.
288 However, when ray width and height is plotted, it is evident that there is some significant
289 overlap in ray size for the small values between the different types (Fig. 6). Although the
290 wood of the second (DBW6) and third (DBW5) morphotypes can contain respectively higher

291 and broader rays, it also includes rays of small size, similar to those of the first morphotype. It
292 must be noted that all three morphotypes include at least one specimen with almost parallel
293 files of tracheids, suggesting that they correspond to a relatively mature part of the wood, at
294 considerable distance from the pith.

295 A similar type of variation in wood anatomy is known to occur in *Pitus*, which represents
296 the best point of comparison despite the fact that the new specimens probably belong to a
297 different genus (see next §). Gordon (1935) differentiated *Pitus* species by the width of their
298 rays (maximum and average size) and the shape of the tracheids (straight or curved). He
299 indicated that “beyond the immediate neighbourhood of the medulla” the rays in all species
300 were relatively constant in width. Ray height in *Pitus* wood has also been observed at various
301 distances from the pith in a trunk of *P. withami* from the Viséan of Scotland (Galtier and
302 Scott, 1994). Although the maximum height increases toward the periphery of the trunk, the
303 average ray height remains the same and was thus identified as a potentially useful taxonomic
304 character within the genus. More recently, Henderson and Falcon-Lang (2011) conducted a
305 principal component analysis on 34 Early Mississippian specimens of *Pitus* from Scotland to
306 separate phylogenetic from ontogenetic variations in wood anatomy. The analysis included
307 not only characters of the rays, such as height and width, cell dimension, and ray density, but
308 also tracheid diameter and the number of rows of radial pits. It revealed the presence of six
309 distinct wood morphotypes, which were interpreted by the authors as representing at least
310 three biological taxa. On the basis of these previous works on *Pitus*, it seems questionable to
311 consider that the three wood morphotypes from the Ducabrook Formation are simply
312 ontogenetic variants of a single taxon, especially given the lack of information on the primary
313 vascular anatomy corresponding to each type of wood. Thus, we propose that the three wood
314 morphotypes be interpreted as evidence of the presence of three taxa.

315

316 3.2.2. *Mississippian taxa with similar types of wood (Table 2)*

317 Several Mississippian taxa from Europe, North America, North Africa, and Australia have
318 secondary xylem generally similar to the Drummond Basin specimens, with araucarian radial
319 pitting, araucarioid cross-field pitting, and multiseriate parenchymatous rays. Isolated pieces
320 of wood with this anatomy are assigned by some workers to the morphogenus *Dadoxylon*
321 Endlicher—in contrast to similar woods with only uniseriate rays, which are assigned to
322 *Agathoxylon* Hartig (= *Araucarioxylon*, see Rößler et al., 2014). At least eight Mississippian
323 genera of stems with this type of wood anatomy have been recognised to date: *Ahnetia*
324 (Decombeix and Galtier, 2017), *Archaeopitys* (Scott and Jeffrey, 1914), *Cauloxylon* (Cribbs,
325 1939), *Eristophyton* (Scott, 1902; Lacey, 1953; Galtier and Scott, 1990; Decombeix et al.,
326 2007, 2008), *Faironia* (Decombeix et al., 2006), *Megalomyelon* (Cribbs, 1940), *Picnoxylon*
327 (Cribbs, 1938) and *Pitus* (Gordon, 1935). Ray size in these taxa and in isolated pieces of
328 wood, such as ‘*Dadoxylon*’ *ambiguum* and *Paleoxylon bourbachensis*, were compared to
329 those of the specimens from the Ducabrook Formation (Table 2). DBW2, which has the
330 lowest and narrowest rays, is most similar to the secondary xylem of *Eristophyton fasciculare*
331 and of *Dadoxylon ambiguum* (Scott, 1902; Galtier and Scott, 1990; Galtier et al., 1998).
332 DBW6, representing the most abundant morphotype among the Ducabrook specimens, is
333 most similar to *Paleoxylon bourbachensis*. This species has been compared to *Pitus withami*
334 by Galtier et al. (1998) but on average its rays are slightly taller and broader. Finally, DBW5
335 and DBW8, characterised by very wide rays, are most similar to the wood of *Pitus dayi*
336 (Gordon, 1935). The only taxon with wood similar to some of the Drummond Basin
337 specimens described in detail from Australia (MSM11) has a ray size similar to specimens of
338 the DBW6 type (Decombeix et al., 2011b, see also below).

339

340 3.2.3. *Importance of the specimens preserving vascular traces to lateral appendages*

341 Specimens DBW4, DBW6, and DBW9 are the only specimens providing information on
342 the primary structure of some of the lignophyte trees preserved in the Ducabrook Formation.
343 How do their features compare to those of previously described Mississippian arborescent
344 lignophytes?

345 The primary vascular structure of DBW4 is characterised by a stele with numerous, small,
346 endarch to mesarch primary xylem strands and departing leaf traces. Because the pith is not
347 preserved, it is not possible to exclude the presence of medullary and/or peri-medullary
348 primary vascular strands. There is also no way to document with certainty the presence of
349 reparatory stands near or facing the departing traces. However, the endarch maturation of
350 some visible strands and departing leaf traces is a notable difference from several arborescent
351 Mississippian genera, including *Pitus* (Scott, 1902; Gordon, 1935; Long, 1979), *Archaeopitys*
352 (Scott and Jeffrey, 2014), *Megalomyelon* (Cribbs, 1940) and *Faironia* (Decombeix et al.,
353 2006), which all have a strictly mesarch maturation. Two other European genera,
354 *Eristophyton* and *Bilignea*, have a maturation that changes from endarch to mesarch at the
355 nodes (Scott, 1924; Decombeix et al., 2007 and references therein); a similar pattern
356 apparently occurs in *Pycnoxylon* from the Tournaisian of Missouri (Cribbs, 1938). This does
357 not seem to be the case in the Australian specimen (DBW4). In *Ahnetia* from the Tournaisian
358 of Algeria (Decombeix and Galtier, 2017), maturation in the largest strands is mesarch,
359 whereas the smallest strands consist only of a few tracheids and maturation is difficult to
360 assess. Genera that have a strictly endarch maturation include *Endoxylon* (Scott, 1924; Lacey,
361 1953) and *Cauloxylon* (Cribbs, 1939). *Endoxylon* can be distinguished from DBW4 by the
362 stele containing only a few large primary xylem strands. In *Cauloxylon*, primary xylem
363 strands are typically in a peri-medullary position, separated from the wood by several layers
364 of parenchyma. However, we should consider that such strands may not have been preserved
365 in DBW4 and that only strands departing as traces are visible. In *Cauloxylon*, however, the

366 departing trace very quickly shows two radially aligned poles of protoxylem, which
367 distinguish this genus from DBW 4, in which only one pole is evident.

368 Sections of DBW4 show, at the same vertical level, groups of closely spaced vascular
369 traces departing to lateral organs (Fig. 5). Superficially, this might suggest an artefact due to
370 compression of the axis and might be a deformation of the central part. However, that this
371 pattern might relate to the true organotaxis is supported by the existence of two other
372 specimens showing a similar organisation, one from the same locality (DBW6) and one
373 described previously from Lower Mississippian strata of the nearby Burdekin Basin
374 (Decombeix et al., 2011b; see Fig 1). These two specimens have a secondary xylem anatomy
375 similar to that of DBW4. DBW6 is a wood fragment that, in its most internal part, has a group
376 of three small vascular traces that are very closely spaced (Plate II, 5). The secondary xylem
377 surrounding these traces shows no significant deformation and there is no doubt that the close
378 arrangement of the traces is not an artefact. This supports the contention that groups of traces
379 are emitted in some of the woody plants from the Ducabrook Formation. The specimen from
380 the Burdekin Basin (MSM11 of Decombeix et al., 2011b) has a preservation similar to DBW
381 6, i.e., its central part is present but not preserved. It also shows the emission of closely
382 located traces at some levels and its secondary xylem anatomy is similar to that of DBW4 (see
383 Table 2). Based on this evidence, two hypotheses need to be considered: (1) that these plants
384 had a complex organotaxis with multiple spirals, or (2) that several vascular traces supplied a
385 single lateral organ. The vascularisation of a single lateral organ by multiple traces is
386 documented in several Mississippian (pro)gymnosperm taxa. The non-arborescent
387 calamopityalean seed ferns *Diichnia* (Beck et al., 1992) and *Triichnia* (Galtier and Beck,
388 1992), respectively, have double and triple vascular traces to their leaves. Similarly, *Faironia*,
389 which has characters of both arborescent (e.g., *Pitrus*) and non-arborescent (e.g.,
390 Calamopityales) Mississippian taxa, produced pairs of traces that divided and vascularised a

391 single petiole in the cortex (Decombeix et al., 2006). *Cauloxylon*, *Picnoxylon* and
392 *Megalomyelon*, three (pro)gymnosperms trees from the Early Mississippian of Missouri, also
393 have vascular traces apparently emitted in pairs (Cribbs, 1938, 1939, 1940). Because these
394 traces were rapidly occluded in the wood of the trunks, it is uncertain whether they
395 vascularised a single organ. With the exception of the calamopityean *Triichnia*, which has a
396 very different wood from the Ducabrook Formation specimens (Galtier and Beck, 1992),
397 *Megalomyelon* is the only taxon in which some groups contain more than two traces (Cribbs,
398 1940). However, it differs from the Australian specimens by its mesarch maturation and its
399 mostly uniseriate to partly biseriate rays. Thus, the information available from DBW4 and
400 DBW6 does not allow their confident assignment to any previously described taxon of
401 Mississippian (pro)gymnosperm.

402 The third specimen providing information on the primary vascular structure of the trees
403 from the Ducabrook Formation is DBW9. The lack of immersed strands either in the
404 medullary or peri-medullary regions of its pith rules out an affinity with *Ahnetia*,
405 *Archaeopitys*, *Cauloxylon*, *Eristophyton waltonii*, *Faironia*, *Megalomyelon*, *Picnoxylon* or
406 *Pitus* (Scott and Jeffrey, 1914; Cribbs, 1939, 1939, 1940; Lacey, 1953; Decombeix et al.,
407 2006; Decombeix and Galtier, 2017). The lack of tracheids in the pith also distinguishes it
408 from *Biliginea* (Scott, 1924). Moreover, the small size of the primary xylem strands
409 distinguishes it from *Endoxylon* and from *Eristophyton fasciculare*, *E. beneirtianum* and *E.*
410 *feisti*. Such very small strands occur in *E. waltonii* and *Ahnetia* but, as mentioned above, other
411 characters including the location of the strands rule out any affinity with these taxa. Thus, the
412 information available on the primary vascular anatomy indicates that DBW9, like DBW4 and
413 DBW6, is both distinct from *Pitus* and not assignable with confidence at this stage to any
414 other previously described Mississippian lignophyte genus.

415

416 3.2.4. *Summary*

417 Woods from the base of the Ducabrook Formation in the Drummond Basin can be assigned to
418 three morphotypes based on ray size. Some information on the primary vascular structure is
419 available for one of these morphotypes and possibly a second. No primary vascular
420 information is available for the morphotype with very broad rays. The specimens have a
421 secondary xylem anatomy similar to that of some coeval arborescent lignophytes reported
422 previously from Europe and North America, such as *Eristophyton* and *Pitus*, but the
423 information available on their primary anatomy does not permit their assignment to
424 established species. At this stage, we do not formalise new taxa for the woody plants from the
425 Ducabrook Formation, because we consider that additional axes with more anatomical
426 characters preserved are required to fully circumscribe their features.

427

428 **4. Trunks from the Yarrol Basin**

429 **4.1. Descriptions**

430 The two available specimens appear similar for all observed characters and are thus
431 described together. In cross-section, the centre of the trunks is composed of a broad
432 parenchymatous pith (Fig. 7) with numerous small primary xylem strands distributed in a
433 peri-medullary position. The preserved secondary xylem is up to 5.5 cm thick. Tissues
434 centrifugal to the secondary xylem are not preserved.

435

436 **4.1.1. Pith (Plate IV; Fig. 7)**

437 The pith is elliptical, about 30 × 25 mm in YB1 and 35 × 25 mm in YB2, and its tissues are
438 extremely well-preserved. It is composed of parenchymatous cells, some with a conspicuous
439 dark content (Plate IV, 1, 2). The parenchyma cells are polygonal, with an average diameter
440 of 151 µm (84–229 µm). Most are slightly elongate radially except in the center of the pith

441 where they are isodiametric. The cells with dark content are distributed randomly within the
442 pith and represent about 1/25 of the pith cells. In some cases, the content appears as a
443 reticulum slightly detached from the cell walls (Plate IV, 2). Many of the dark cells show
444 evidence of derivation from a common mother cell and occur in pairs (Plate IV, 2). The
445 divisions appear to occur variably in the radial or tangential plane.

446

447 *4.1.2. Primary vascular anatomy and vascular traces to lateral organs (Plate IV, V; Fig. 7, 8)*

448 The contact zone between the pith and the secondary xylem is not preserved throughout the
449 circumference of the specimens (e.g., Fig. 7; Plate IV, 1) so the complete architecture of the
450 primary vascular system could not be reconstructed. However, observations of the best
451 preserved parts of YB1 and YB2 provide valuable information on the primary xylem and
452 departing leaf traces. Primary xylem strands form a ring in the outermost part of the pith (Fig.
453 8; Plate IV, 3). About 35–40 strands are distributed around the circumference of the pith in
454 YB1. Given the existence of non-preserved zones, the original number is estimated to be
455 closer to 50. Primary xylem strands are positioned 1–2 mm apart (Fig. 8; Plate IV, 3). Their
456 size and shape are highly variable, as is their distance to the secondary xylem and to adjacent
457 strands (Fig. 8; Plate IV, 3–5). This variability is probably due to significant changes in strand
458 size, location, and number in the zones of incipient leaf trace emission. The smallest strands
459 are composed of a few tracheids and are about 100 μm wide or less. They are typically
460 separated from the secondary xylem by 5–7 parenchyma cells (Plate IV, 3, 4). The largest
461 strands are about 200 μm in diameter (Plate IV, 5, 6). There is some evidence of strand
462 division. Some primary xylem strands have 1–3 tracheids of smaller diameter interpreted as
463 protoxylem tracheids, and the maturation in most cases appears to be endarch (Plate IV, 4),
464 although some of the largest strands have a more mesarch appearance. In other strands, it is
465 impossible to clearly identify the protoxylem.

466 Several vascular traces departing to lateral organs are evident in the peels and thin-sections
467 (Plate IV, 5; Plate V; Fig. 7; Fig. 8). A general view of the trunk YB2 shows two relatively
468 close traces in the wood (Fig. 7, arrows top left). Two other, much less advanced, departing
469 traces are visible in the right part of the specimen and form a 140° angle with the previous
470 two. The distance between two traces of a pair is about 5 mm and a closer examination shows
471 that one of the two traces is slightly more advanced than the other. The other regions of the
472 pith-secondary xylem boundary are not well preserved; thus, it is impossible to follow leaf
473 trace emission on that specimen. Investigation of YB1 provides crucial additional
474 information. Several leaf traces at different stages of emission can be seen on a given cross-
475 section. They are usually 4–6 mm apart and separated by a few very small strands composed
476 of a few tracheids (Fig. 8). The occurrence of pairs of traces noted on YB2 is supported by the
477 presence of ‘successive’ traces at a relatively similar stage of emission (T1, T2 in Fig. 8B).
478 However, it is not entirely certain that this is a consistent pattern owing to the incompleteness
479 of the primary xylem zone around the circumference of the pith in both specimens.

480 Although some features are not entirely clear, general stages of leaf trace emission can be
481 recognised from the observation of several sections. The first recognizable stage of leaf trace
482 production is the enlargement and division of an immersed primary xylem strand. This leads
483 to the formation of a larger, broadly triangular strand that moves closer to the secondary
484 xylem (Fig. 8; Plate V, 1). Files of secondary xylem tracheids take on a curved aspect where
485 the leaf trace is going to be emitted. At a more advanced stage, the strand divides radially and
486 a complex of primary xylem strands is formed in the zone facing the location of the leaf trace
487 departure (Fig. 8; Plate V, 2, 3, 5, 6, red arrowheads). There is a conspicuous neighbour strand
488 about 100 µm wide orientated slightly obliquely about 1 mm from the trace (Fig. 8; Plate V,
489 1, 2, 3, yellow arrowheads). A group of a few tracheids is also present on the other side of the
490 incipient leaf trace but it is much less conspicuous and not visible in all cases (Fig. 8; Plate V,

491 3). At an even more advanced stage, the departing leaf trace contains three radially aligned
492 protoxylem strands protruding through the secondary xylem (Fig. 8; Plate IV, 5; Plate V, 4,
493 7). The trace is then about 1.2×0.5 mm in major dimensions, much larger than the largest
494 primary xylem strands (Plate IV, 5; Plate V, 4). As the leaf trace departs, the neighbor strand
495 moves a little more to the side but remains clearly present, and the small strands of primary
496 xylem composed of a few tracheids that were facing the trace (Plate V, 2, 5) apparently
497 disappear (Plate V, 4). Although a lateral strand located about 1 mm from the site of the leaf
498 trace emission is a constant feature in all departing traces that we observed, its origin and
499 relation to the leaf trace remains uncertain. It is present in the earliest stages of leaf trace
500 emission and it is unclear whether it (1) results from a division of the large strand that gives
501 off the trace (reparatory strand), (2) results from the increase in size of a previously non-
502 detected strand composed of a few tracheids, or (3) arises *de novo*.

503

504 4.1.3. Secondary xylem (Plate VI)

505 The secondary xylem consists of tracheids and multiseriate parenchymatous rays (Plate VI,
506 1–3). In cross-section, the wood shows some growth ring boundaries (Plate VI, 3). The best
507 preserved rings are 3–7 mm in width. False rings, characterised by 3–5 rows of tracheids with
508 a reduced radial diameter, are also present sporadically. The secondary xylem tracheids are
509 polygonal in cross-section and $17\text{--}75$ μm in diameter. The rays are long; some cross the entire
510 wood cylinder. They separate 2–10 files of tracheids and are expanded in the pith region by
511 enlargement of the cells (Plate VI, 1–3).

512 Tracheids are not pitted on their tangential walls. The rays are 2–5 cells wide in tangential
513 section and up to 60 cells high (Plate VI, 4–5). The average size for 100 measured rays is 2.7
514 cells wide and 14 cells high. Ray cells are circular to polygonal in tangential longitudinal
515 section, with variable sizes. They are 32 ($16\text{--}53$) μm wide and 55 ($30\text{--}79$) μm high.

516 In radial longitudinal section, tracheid walls bear 1–4 rows of pits that are hexagonal to
517 circular (Plate VI, 6–7). The pits cover the entire width of the radial walls. Almost 80% of
518 tracheids have two or three rows of pits, which are always arranged alternately. They measure
519 14 μm (10–20 μm , $n=30$) in diameter and have an oblique, slit-like to oval aperture (Plate VI,
520 7). Ray cells are 81–257 μm long with vertical walls. There are no ray tracheids. Cross-fields
521 bear araucarioid pitting, with 6–12 crowded oval to circular pits (Plate VI, 8).

522

523 4.2. *Affinities*

524 The Yarrol Basin trunks are characterised by (1) a large parenchymatous pith, (2)
525 numerous small primary xylem strands in a peri-medullary position, (3) leaf traces probably
526 emitted in pairs, much larger than the primary xylem strands, and containing three radially
527 aligned protoxylem strands as they depart from the stele, and (4) secondary wood with
528 multiseriate rays, araucarian radial pitting and araucarioid cross-field pitting. *Ahnetia*
529 (Decombeix and Galtier, 2017), *Archaeopitys* (Scott and Jeffrey, 1914), *Cauloxylon* (Cribbs,
530 1939), *Eristophyton waltonii* (Lacey, 1953; Galtier and Scott, 1990), *Faironia* (Decombeix et
531 al., 2006), *Megalomyelon* (Cribbs, 1940), *Picnoxylon* (Cribbs, 1938) and *Pitus* (Gordon,
532 1935) share with the new trunks the presence of a parenchymatous eustele with numerous
533 small primary xylem strands in a peri-medullary position. Two main characters distinguishing
534 the Australian trunks from *Archaeopitys*, *Faironia*, *Megalomyelon* and *Pitus* are the presence
535 of endarch maturation in most strands and the presence of several radially aligned strands in
536 the departing vascular trace to lateral appendages. An additional difference from *Archaeopitys*
537 and *Pitus* is the lack of true medullary strands in the Australian trunks; however, although this
538 condition has been recorded in all species of *Pitus*, it is not necessarily represented in all
539 specimens of that genus (Gordon, 1935). Both *Picnoxylon* and *Eristophyton waltonii* have a
540 maturation that changes from endarch between nodes to mesarch at the nodes (Cribbs, 1938;

541 Lacey, 1953). Although this is more similar to the maturation in the Yarrol Basin trunks, the
542 latter can again be distinguished by their more complex leaf traces.

543 *Ahnetia* from the Mississippian of Algeria (Decombeix and Galtier, 2017) has some
544 similarities with the specimens from the Yarrol Basin, including the presence of small peri-
545 medullary primary xylem strands, a complex production of leaf traces, and a wood with rays
546 that are 1–5 cells wide and 1–50 cells high. On the other hand, *Ahnetia* differs significantly
547 from the new specimens by the greater distance between strands (about 6 mm), and its smaller
548 leaf traces with a single protoxylem strand. There is also no evidence of pairs of traces in
549 *Ahnetia*. It is notable, however, that the stages of primary xylem strand changes leading to
550 leaf trace production in *Ahnetia* are quite similar to those of the new specimens, including the
551 formation of a large triangular primary xylem strand with several protoxylem poles and the
552 presence of a conspicuous lateral strand, whose origin in *Ahnetia* remains unclear.

553 Finally, *Cauloxylon* from the late Tournaisian of Missouri (Cribbs, 1939) shares some
554 important characters with the new specimens, including much reduced primary xylem strands
555 (2–4 tracheids in some cases), endarch maturation even in some large strands, complex
556 branching of strands prior to leaf trace departure, the occurrence of paired traces separated by
557 a few small strands, and the presence of more than one protoxylem strand in the departing
558 trace. The secondary xylem of *Cauloxylon* is also broadly similar to that of the Australian
559 trunks, but the rays are a larger (1–7) and taller (commonly 30–40 cells tall versus an average
560 of 14 for the Australian trunks). However, *Cauloxylon* also differs from the Australian trunks
561 by several characters, including the presence of sclerotic nests in the pith, the presence of two
562 radially aligned poles of protoxylem in the departing trace, versus three in the Australian
563 trunks, and smaller traces (200–400 μm).

564 Although the new trunks from the Yarrol Basin share several significant characters with
565 arborescent lignophytes from Europe, North America and North Africa they do not appear to

566 fit the diagnosis of any genus described previously. They might, however, belong to a group
567 of Mississippian trees with a complex primary vascular architecture that includes taxa such as
568 *Cauloxylon* or *Ahnetia* from the late Tournaisian of USA and Algeria, respectively. It is
569 interesting to note that this type of complex primary vascular organisation has not been
570 described previously in Viséan taxa.

571 It should be noted that although Carboniferous woody axes with a preserved pith and
572 primary vascular system have been reported in South America, they are younger than the
573 other taxa mentioned here (Late Mississippian or Pennsylvanian) and typically comprise
574 wood with uniseriate rays and a much more simple organization of the primary xylem and leaf
575 traces (e.g., Pujana, 2005; Pujana and Césari, 2008).

576 Cells with marginally contracted dark contents (Plate IV, 2), commonly in the form of a
577 three-dimensional filamentous reticulum, have been noted from a diverse range of woods and
578 rhizomes of Carboniferous to Cretaceous age in several earlier studies (e.g., Andrews and
579 Lenz, 1943; Smoot and Taylor, 1983; Tidwell and Herbert, 1992; Weaver et al., 1997; Strullu-
580 Derrien et al., 2012; McLoughlin and Strullu, 2016; Krings et al., 2017). Their filamentous
581 character is reminiscent of fungal hyphae, but they may alternatively represent biomimetic
582 mineral precipitates (Klymiuk et al., 2013), some of which may have been mediated by
583 various bacterial groups during early diagenesis (Konhauser, 1997; Baumgartner et al., 2006;
584 Krings et al., 2017). They appear to have no significance for systematic placement of the
585 Yarrol Basin woods.

586

587 ***4.3. Systematic palaeobotany***

588 Unranked clade: Lignophytia Kenrick and Crane 1997.

589 Class, order and family: Incertae sedis.

590 ***Ninsaria* Decombeix, Galtier, McLoughlin, Meyer-Berthaud gen. nov.**

591 *Type species: Ninsaria australiana* Decombeix, Galtier, McLoughlin, Meyer-Berthaud sp.
592 nov. (here designated).

593 *Generic diagnosis:* Stem with primary and secondary vascular tissues. Eustele consisting of
594 numerous small discrete strands of primary xylem at the periphery of a broad parenchymatous
595 pith. Primary xylem strands in peri-medullar position, composed of a few tracheids. Leaf trace
596 emission starting with two divisions of a primary xylem strand and formation of an arc-
597 shaped group of three strands that progresses towards the secondary xylem. Departing leaf
598 trace much larger than axial strands, with three radially aligned protoxylem strands. Leaves
599 arranged in a complex spiral. Secondary xylem tracheids with multiseriate araucarioid
600 bordered pits on radial walls. Cross-field pitting araucarioid. Rays multiseriate, of medium
601 height.

602 *Etymology:* After Ninsar, the Sumerian goddess of plants.

603 ***Ninsaria australiana* Decombeix, Galtier, McLoughlin, Meyer-Berthaud sp. nov**

604 *Holotype:* YB1, Plates IV, V (2–7), VI.

605 *Paratype:* YB2, Plate V(1).

606 *Stratigraphic and geographic occurrence:* Unnamed bed within the Rockhampton Group
607 between the Lion Creek Limestone and Lorrain Formation; from exposures between localities
608 UQL4887 and UQL4981 of Webb (1990).

609 *Age:* late Viséan.

610 *Etymology:* After Australia, reflecting the geographic origin of the specimens.

611 *Specific diagnosis:* Stem with a 20–30 mm wide eustele, composed of 40–50 axial strands and
612 incipient leaf traces. Pith of polygonal parenchyma cells, some with dark reticulate content.
613 Primary xylem strands peri-medullar, separated from the secondary xylem by several layers of
614 parenchyma cells. Distance between strands 1–2 mm. Primary xylem strands small, typically
615 <200 µm in diameter, and usually consisting of a few tracheids. Xylem maturation endarch in

616 small strands. Leaf trace about 1.2×0.5 mm. Tracheids of secondary xylem rectangular to
617 polygonal, with average diameter equal to, or slightly larger than, the metaxylem tracheids.
618 Rays up to five cells wide, up to 60 cells in height.

619

620 **5. (Pro)gymnosperm trees in the Mississippian of Australia**

621 The present work has shown that several taxa with *Pitus*-like wood, i.e., with araucarian
622 pitting and multiseriate rays, are present in Mississippian deposits of Australia. Specimens
623 from the Viséan of the Drummond Basin, like middle Tournaisian specimens reported
624 previously from the Burdekin Basin (Decombeix et al., 2011b) differ from *Pitus* at least by
625 their phyllotaxis. Trunks from the Yarrol Basin also differ from *Pitus*, in this case by several
626 characters of their primary vascular architecture and leaf trace anatomy. All these new
627 specimens appear to be different from previously described species of Mississippian
628 lignophytes. In summary, these examples of taxa with ‘*Pitus*-like wood’ from Australia: (1)
629 are actually distinct from *Pitus*; (2) correspond to more than one taxon; and (3) differ in
630 characters of their primary vascular organisation from Mississippian taxa with a similar wood
631 anatomy currently known from Europe, North America and North Africa (Galtier and Meyer-
632 Berthaud, 2006). These results do not imply the absence of *Pitus* in the Mississippian of
633 Australia, because other specimens with a similar type of wood have been reported for which
634 the anatomy of the primary vascular system remains unknown. However, the specimens from
635 the Drummond and Yarrol basins reveal that the taxonomic diversity of trees with this general
636 type of wood in Australia is higher than initially suspected. This diversity supports previous
637 observations that eastern Australia saw a change in lignophyte tree diversity around the
638 Devonian–Carboniferous boundary similar to that recorded in Laurussia, with the extinction
639 of the arborescent progymnosperm *Archaeopteris* that dominated Late Devonian forests and

640 the diversification of new taxa of (pro)gymnosperm trees during the Early and Middle
641 Mississippian (Decombeix et al., 2011a).

642 The occurrence of at least one arborescent species, the progymnosperm *Protopitys* both in
643 Australia and Europe during the middle Tournaisian (Decombeix et al., 2011b, 2015) provides
644 palaeontological evidence of floristic exchange between Gondwana and Laurussia around the
645 Devonian–Mississippian transition. Anatomically preserved plants of smaller size from the
646 locality of Ruxton (northeastern Queensland) also reveal some similarities at least at the
647 generic level between Australian and European taxa (Galtier et al., 2007). There are, however,
648 also several examples of Tournaisian plant genera known only from Australia, such as the
649 arborescent zygopterid fern *Symplocopteris* (Hueber and Galtier, 2002) and the ovulate organ
650 *Ruxtonia* (Galtier et al., 2007). For the Viséan, the trees with *Pitus*-like wood from the
651 Drummond and Yarrol basins represent new examples of plants that are presently documented
652 only in Australia. In this context, it is interesting to note that eastern Australia saw a change
653 from more cosmopolitan conodonts in the Tournaisian to more endemic conodonts in the
654 Viséan, whereas the Viséan corals are clearly endemic; other Viséan marine taxa are,
655 however, considered more cosmopolitan (e.g., Jones et al., 2000; Webb, 2000; Denayer and
656 Webb, 2015)

657 Morris (1985) considered that, during the Viséan, *Pitus*-like trees formed ombrophile
658 forests with a tree-fern understorey and that this indicated a more humid climate in eastern
659 Australia than during the Tournaisian. This interpretation was based on (1) the association of
660 “*Pitus*” and the zygopteridalean tree-fern *Austroclepsis australis* (Sahni, 1932) in the Viséan
661 of New South Wales, and (2) the fact that tree rings in known specimens of ‘*Pitus*’ were
662 either indistinct or completely absent. The co-occurrence of lignophyte trees with a *Pitus* type
663 of wood and zygopteridalean tree ferns has now also been documented in the middle
664 Tournaisian locality of Dotswood in the Burdekin Basin (Hueber and Galtier, 2002;

665 Decombeix et al., 2011b) and these ferns are also present in the Drummond Basin (S.
666 McLoughlin, unpub. data). This association can thus be found earlier than the Viséan and is
667 not typical of that age, although the respective taxa of ferns and lignophyte trees might differ
668 between assemblages. No arborescent fern (Zygopteridales or other) is known in the
669 Mississippian of Laurussia, so this association appears to be distinctive to eastern Australia.

670 Regarding growth parameters, woods from both the Ducabrook Formation (Viséan) and
671 the Yarrol Basin (late Viséan) have distinct growth ring boundaries, which implies that their
672 growth was seasonal. This is particularly interesting when compared to the older specimens
673 from the middle Tournaisian of the Burdekin Basin in which growth rings are much more
674 subtle (Decombeix et al., 2011b; Laloux, unpub. data). This difference could be due to the
675 combined effect of (1) the southward movement of Australia during the Mississippian from
676 tropical to temperate latitudes, and (2) the onset of the Late Paleozoic Ice Age in western
677 Gondwana during the Viséan (e.g., Caputo et al., 2008; Gulbranson et al., 2010). However,
678 only small portions of wood are known from the Drummond and Yarrol basins and, in some
679 cases, they represent the inner part of the trunk, a region for which growth ring anatomy
680 might reflect developmental processes in addition to cambial reaction to environmental
681 constraints. Thus, it is difficult to analyze the possible climatic information provided by those
682 rings in more detail. A warm Viséan interval in Australia has been suggested based on several
683 proxies including compression/impression floras (Iannuzzi & Pfefferkorn, 2002) and reef
684 history (Webb, 2002). The apparently more seasonal growth of the Viséan trees compared to
685 the Tournaisian ones might thus also be linked to a different biology and/or to a different
686 habitat of origin, as the trunks are not found in situ.

687

688 **6. Conclusions**

689 New permineralised plants with a *Pitus* type of wood are described from the Drummond and
690 Yarrol basins of Queensland, Australia. The woods represent several distinct morphotaxa and
691 the available information on their primary vascular system indicates that they differ from
692 *Pitus* and from other previously described taxa of Mississippian lignophytes. These new
693 specimens increase the known diversity of woody plants in Australia during the Mississippian
694 and show that the floras of the region at this time were more complex than is usually
695 interpreted based on compression/impression specimens.

696

697 **Acknowledgements**

698 We thank Pam Wilson and Kristin Spring (Queensland Museum) for their help with the loan.
699 ALD and BMB acknowledge funding from LabEx CeMEB (Exploratory Project MARCON)
700 during the course of this research. Financial support to Stephen McLoughlin by the Swedish
701 Research Council (VR grant 2014-5234) and National Science Foundation (project #1636625)
702 is gratefully acknowledged. AMAP (Botany and Computational Plant Architecture) is a joint
703 research unit which associates CIRAD (UMR51), CNRS (UMR5120), INRA (UMR931),
704 IRD (R123), and Montpellier University (UM); <http://amap.cirad.fr>

705

706 **References**

707 Anderson, J.M., Anderson, H.M., Archangelsky, S., Bamford, M.K., Chandra, S., Dettmann,
708 M., Hill, R., McLoughlin, S., Rösler, O., 1999. Patterns of Gondwana plant colonisation
709 and diversification. *J. Afr. Earth Sci.* 28, 145–167.

710 Andrews, H.N., Lenz, L.W., 1943. A mycorrhizome from the Carboniferous of Illinois. *Bull.*
711 *Torrey Bot. Club* 70, 120–125.

- 712 Baumgartner, L.K., Reid, R.P., Dupraz, C., Decho, A.W., Buckley, D.H., Spear, J.R.,
713 Przekop, K.M., Visscher, P.T., 2006. Sulphate reducing bacteria in microbial mats:
714 Changing paradigms, new discoveries. *Sediment. Geol.* 185, 131–145.
- 715 Blake, P.R., Withnall, I.W., Fitzell, M.J., Kyriazis, Z., Purdy, D.J., 2012. Geology of the
716 western part of the Drummond Basin. *Queensland Geological Record* 2012/17
- 717 Beck, C.B., Galtier, J., Stein, W.E. Jr., 1992. A reinvestigation of *Diichnia* Read from the
718 New Albany Shale of Kentucky. *Rev. Palaeobot. Palynol.* 75, 1–32.
- 719 Caputo, M.V., de Melo, J.H.G., Streef, M., Isbell, J.L., 2008. Late Devonian and Early
720 Carboniferous glacial records in South America. In: Fielding, C.R., Frank, T.D., Isbell,
721 J.L. (Eds.), *Resolving the Late Paleozoic Ice Age in Time and Space*, Geological
722 Society of America, Boulder, CO, pp. 161–174.
- 723 Chapman, F., 1904. On a collection of upper Palaeozoic and Mesozoic fossils from Western
724 Australia and Queensland, in the National Museum, Melbourne. *Proc. R. Soc. Victoria*,
725 N.S., 16, 306–335.
- 726 Cook, A., Rozefelds, A., 2015. *In Search of Ancient Queensland*. Queensland Museum,
727 Brisbane, 277 pp.
- 728 Cribbs, J.E., 1938. A new fossil plant from the Reed Spring Formation of southwestern
729 Missouri. *Am. J. Bot.* 25, 311–321.
- 730 Cribbs, J.E., 1939. *Cauloxylon ambiguum*, gen. et sp. nov., a new fossil plant from the Reed
731 Spring Formation of southwestern Missouri. *Am. J. Bot.* 26, 440–449.
- 732 Cribbs, J.E., 1940. Structure of fossil stem of pityean affinity from the Reed Springs
733 Formation of Missouri. *Bot. Gaz.* 101, 582–597.
- 734 Davis, B.K., Henderson, R.A., 1996. Rift-phase extensional fabrics of the back-arc
735 Drummond Basin, eastern Australia. *Basin Res.* 8, 371–381

- 736 Decombeix, A.-L., 2013. Bark anatomy of an Early Carboniferous tree from Australia. *IAWA*
737 *J.* 34, 183–196.
- 738 Decombeix, A.-L., Galtier, J., 2017. *Ahnetia*, a new lignophyte stem from the Lower
739 Carboniferous of southern Algeria. *Rev. Palaeobot. Palynol.* 237, 62–74.
- 740 Decombeix, A.-L., Galtier, J., Meyer-Berthaud, B., 2006. *Faironia difasciculata*, a new
741 gymnosperm from the Early Carboniferous (Mississippian) of Montagne Noire, France.
742 *Rev. Palaeobot. Palynol.* 142, 79–92.
- 743 Decombeix, A.-L., Meyer-Berthaud, B., Galtier, J., 2007. A review of the genus *Eristophyton*,
744 with special focus on the Mississippian species. *C. R. Palevol* 6, 393–401.
- 745 Decombeix, A.-L., Meyer-Berthaud, B., Galtier, J., 2008. Diversity of Mississippian
746 arborescent lignophytes: a new species of *Eristophyton* from the middle Tournaisian of
747 France. *Int. J. Plant Sci.* 169, 1116–1127.
- 748 Decombeix, A.-L., Meyer-Berthaud, B., Galtier, J., 2011a. Transitional changes in
749 arborescent lignophytes at the Devonian–Carboniferous boundary. *J. Geol. Soc. London*
750 168, 547–557.
- 751 Decombeix, A.-L., Meyer-Berthaud, B., Galtier, J., Talent, J.A., Mawson, R., 2011b.
752 Arborescent lignophytes in the Tournaisian vegetation of Queensland (Australia):
753 Palaeoecological and palaeogeographical significance. *Palaeogeogr. Palaeoclimatol.*
754 *Palaeoecol.* 301, 39–55.
- 755 Decombeix, A.-L., Galtier, J., Prestianni, C., 2015. The Early Carboniferous progymnosperm
756 *Protopytis*: new data on vegetative and fertile structures, and on its geographic
757 distribution. *Hist. Biol.* 27, 345–354.
- 758 Denayer, J., Webb, G.E., 2015. *Cionodendron* and related lithostrotonid genera from the
759 Mississippian of eastern Australia: systematics, stratigraphy and evolution. *Alcheringa*
760 39, 315–376.

- 761 Dunn, M.T. 2006. A review of permineralized seed fern stems of the upper Paleozoic. J.
762 Torrey Bot. Soc. 133, 20–32.
- 763 Falcon-Lang, H. J., Galtier, J., 2010. Anatomically-preserved tree-trunks in late Mississippian
764 (Serpukhovian, late Pendleian-Arnsbergian) braided fluvial channel facies, near
765 Searston, southwest Newfoundland, Canada. Rev. Palaeobot. Palynol. 160, 154–162.
- 766 Fleming, P.J.G., 1967. Names for Carboniferous and Permian formations. Qd Govt. Mining J.
767 68, 113–116.
- 768 Galtier, J., 1988. Morphology and phylogenetic relationships of early pteridosperms. *In*: Beck,
769 C.B. (Ed.) Origin and Evolution of Gymnosperms. Columbia University Press, New
770 York, pp. 135–176.
- 771 Galtier, J., 2002. *Pitus*, a giant tree of the Early Carboniferous time. *In*: Dernbach, U.,
772 Tidwell, W.D. (Eds.), Secrets of Petrified Plants. Fascination from Millions of Years.
773 D'Oro Publ., Heppenheim, Germany, pp. 34–37.
- 774 Galtier, J., Beck, C.B., 1992 *Triichnia*, a new eustelic calamopityacean from the Lower
775 Carboniferous of France. Palaeontographica 224B, 1–16.
- 776 Galtier, J., Scott, A.C., 1985. Diversification of early ferns. Proc. R. Soc. Edinb. 86, 289–301.
- 777 Galtier, J., Scott, A.C., 1990. On *Eristophyton* and other gymnosperms from the Lower
778 Carboniferous of Castleton Bay, East Lothian, Scotland. Geobios 23, 5–19.
- 779 Galtier, J., Scott, A.C., 1994. Arborescent gymnosperms from the Visean of East Kirkton,
780 West Lothian, Scotland. Tran. R. Soc. Edinb. 84, 261–266.
- 781 Galtier, J., Phillips, T.L., 1999. The acetate peel technique. *In*: Jones, T.P., Rowe, N.P. (Eds.),
782 Fossil Plants and Spores: Modern Techniques. The Geological Society, London, pp. 67–
783 70.
- 784 Galtier, J., Meyer-Berthaud, B., 2006. The diversification of early arborescent seed ferns. J.
785 Torrey Bot. Soc. 133, 7–19.

- 786 Galtier, J., Schneider, J.-L., Grauvogel-Stamm, L., 1998. Arborescent gymnosperms and the
787 occurrence of *Protopitys* from the Lower Carboniferous of the Vosges, France. Rev.
788 Palaeobot. Palynol. 99, 203–215.
- 789 Galtier, J., Feist, R., Talent, J.A., Meyer-Berthaud, B., 2007. New permineralised flora and
790 trilobites from the mid-Tournaisian (early Carboniferous) Ruxton Formation, Clarke
791 River Basin, northeastern Australia. Palaeontology 50, 223–243.
- 792 Gordon, W.T., 1935. The genus *Pitys*, Witham, emend. Trans. R. Soc. Edinb. 58, 279–311.
- 793 Gould, R.E., 1975. The succession of Australian pre-Tertiary megafossil floras. Bot. Rev. 41,
794 453–483.
- 795 Gulbranson, E.L., Montañez, I.P., Schmitz, M.D., Limarino, C.O., Isbell, J.L., Marensi, S.A.,
796 Crowley, J.L., 2010. High-precision U-Pb calibration of Carboniferous glaciation and
797 climate history, Paganzo Group, NW Argentina. Geol. Society. Amer. Bull. 122, 1480–
798 1498.
- 799 Hass, H., Rowe, N.P., 1999. Thin sections and wafering. In: Jones, T.P., Rowe, N.P. (Eds.),
800 Fossil Plants and Spores: Modern Techniques. The Geological Society, London, pp. 76–
801 81.
- 802 Henderson, E., Falcon-Lang, H.J., 2011. Diversity and ontogeny of *Pitus* tree-trunks in the
803 early Mississippian rocks of the Isle of Bute, Scotland: The importance of sample size
804 and quantitative analysis for fossil wood systematics. Rev. Palaeobot. Palynol. 166,
805 202–212.
- 806 Henderson, R.A., Davis, B.K., Fanning, C.M., 1998. Stratigraphy, age relationships and
807 tectonic setting of rift-phase infill in the Drummond Basin, central Queensland. Aust. J.
808 Earth Sci. 45, 579–595.

809 Hueber, F.M., Galtier, J., 2002. *Symplocopteris wyattii* n. gen. et n. sp.: a zygopterid fern with
810 a false trunk from the Tournaisian (Lower Carboniferous) of Queensland, Australia.
811 Rev. Palaeobot. Palynol. 119, 241–273.

812 Iannuzzi, R., Pfefferkorn, H.W., 2002. A pre-glacial, warm-temperate floral belt in Gondwana
813 (late Visean, Early Carboniferous). PALAIOS 17, 571–590.

814 Jack, R.L., Etheridge, R. Jr., 1892. The geology and palaeontology of Queensland and New
815 Guinea. Geol. Surv. Qd Publ. 72, 1–766.

816 Jell, P.A., 2013. Geology of Queensland. Geological Survey of Queensland, Brisbane, 970 pp.

817 Jenkins, T.B.H., Crane, D.T., Mory, A.J., 1993. Conodont biostratigraphy of the Visean Series
818 in eastern Australia. Alcheringa 17, 211–283.

819 Johnson, S.E., Henderson, R.A., 1991. Tectonic development of the Drummond Basin,
820 eastern Australia: back-arc extension and inversion in a late Paleozoic active margin
821 setting. Basin Res. 3, 197–213.

822 Jones, P.J., 1996. Carboniferous (Chart 5). In: Young, G.C., Laurie J.R. (Eds.), Australian
823 Phanerozoic Timescales. Oxford University Press, Oxford, U.K., pp. 110–126 + chart 5.

824 Jones, P.J., Metcalfe, I., Engel, B.A., Playford, G., Rigby, J., Turner, S., Webb, G.E., 2000.
825 Carboniferous palaeobiogeography in Australasia. In: Wright, A.J., Young, G.C.,
826 Talent, J.A., Laurie, J.R. (Eds.), Palaeobiogeography of Australasian Faunas and Floras,
827 Association of Australasian Palaeontologists Memoir 23, pp. 259– 286.

828 Kenrick, P., Crane, P.R., 1997. The origin and early diversification of land plants: a cladistic
829 study, Smithsonian Institution Press, Washington, DC, 441 pp.

830 Klymiuk, A.A., Harper, C.J, Moore, D.S., Taylor, E.L., Taylor, T.N., Krings, M., 2013.
831 Reinvestigating Carboniferous “actinomycetes”: authigenic formation of biomimetic
832 carbonates provides insight into early diagenesis of permineralized plants. PALAIOS
833 28, 80–92.

- 834 Konhauser, K.O., 1997. Bacterial iron biomineralization in nature. *FEMS Microbiol. Rev.* 20,
835 315–326.
- 836 Krings, M., Harper, C.J., White, J.F., Barthel, M., Heinrichs, J., Taylor, E.L., Taylor, T.N.,
837 2017. Fungi in a *Psaronius* root mantle from the Rotliegend (Asselian, Lower
838 Permian/Cisuralian) of Thuringia, Germany. *Rev. Palaeobot. Palynol.* 239, 14–30.
- 839 Krosch, N.J., Kay, J.R., 1977. Limestone Resources of the Rockhampton region. *Geol. Surv.*
840 *Qd Rep.* 98, 1–72.
- 841 Lacey, W.S., 1953. Scottish Lower Carboniferous Plants: *Eristophyton waltoni* sp. nov. and
842 *Endoxylon zonatum* (Kidston) Scott from Dunbartonshire. *Ann. Bot.* 17, 579–597.
- 843 Long, A.G., 1979. Observations on the Lower Carboniferous genus *Pitus* Witham. *Trans. R.*
844 *Soc. Edinb.* 70, 111–127.
- 845 Maxwell, W.G.H., 1964. The geology of the Yarrol Region. Part 1. Biostratigraphy. *Pap. Dep.*
846 *Geol. Univ. Qd* 5(9), 1–79.
- 847 McKelvey, B.C., McPhie, J., 1985. Tamworth Belt. In: Martinez Diaz, C., (general editor),
848 Wagner, R.H., Winkler Prins, C.F., Granados, L.F. (Eds.), *The Carboniferous of the*
849 *World II. Australia, Indian subcontinent, South Africa, South America, & North*
850 *Africa.* Madrid: Instituto Geologico y Minero de Espana: Empresa Nacional Adaro de
851 *Investigaciones Mineras*, pp. 15–23.
- 852 McLoughlin, S., Strullu-Derrien, C., 2016. Biota and palaeoenvironment of a high middle-
853 latitude Late Triassic peat-forming ecosystem from Hopen, Svalbard Archipelago. In:
854 Kear, B.P., Lindgren, J., Hurum, J.H., Milàn, J., Vajda, V. (Eds.), *Mesozoic Biotas of*
855 *Scandinavia and its Arctic Territories.* Geological Society of London Special
856 *Publications* 434, 87–112.
- 857 Mond, A., 1973. Explanatory Notes on the Dalby 1:250 000 Geological Sheet. Bureau of
858 Mineral Resources, Australia and Geological Survey of Qld, Brisbane, 24 pp.

- 859 Morris, N., 1985. The floral succession in eastern Australia. In: Martinez Diaz, C., (general
860 editor), Wagner, R.H., Winkler Prins, C.F., Granados, L.F. (Eds.), *The Carboniferous*
861 *of the World II. Australia, Indian subcontinent, South Africa, South America, & North*
862 *Africa*. Madrid: Instituto Geologico y Minero de Espana: Empresa Nacional Adaro de
863 *Investigaciones Mineras*, pp. 118–123.
- 864 Murray, C.G., Ferguson, C.L., Flood, P.G., Whitaker, W.G., Korsch, R.J., 1987. Plate tectonic
865 model for the Carboniferous evolution of the New England Fold Belt. *Aust. J. Earth*
866 *Sci.* 34, 213–236.
- 867 Murray, C.G., Blake, P.R., Crouch, S.B.S., Hayward, M.A., Robertson, A.D.C., Simpson,
868 G.A., 2012. Geology of the Yarrol Province central coastal Queensland. *Queensland*
869 *Geol.* 13, 1–675.
- 870 Olgers, F., 1972. The geology of the Drummond Basin. *Bur. Min. Resour., Geol. Geophys.,*
871 *Bull.* 132, 1–78.
- 872 Playford, G., 1978. Lower Carboniferous spores from the Ducabrook Formation, Drummond
873 Basin, Queensland. *Palaeontographica* 167B, 105–160.
- 874 Playford, G., 1985. Palynology of the Australian Lower Carboniferous: a review. *Compte*
875 *Rendu, Dixième Congrès International de Stratigraphie et de Géologie du Carbonifère*
876 4, 247–265.
- 877 Prestianni, C., Rustán, J.J., Balseiro, D., Vaccari, E., Sterren, A.F., Steemans, P., Rubinstein,
878 C., Astini, R.A., 2015. Early seed plants from Western Gondwana:
879 Paleobiogeographical and ecological implications based on Tournaisian (Lower
880 Carboniferous) records from Argentina. *Palaeogeogr. Palaeoclimatol. Palaeoecol.* 417,
881 210–219.

- 882 Pujana, R.R., 2005. Gymnospermous woods from Jejenes Formation, Carboniferous of San
883 Juan, Argentina: *Abietopitys petriellae* (Brea and Césari) nov. comb. Ameghiniana 42,
884 725–731.
- 885 Pujana, R.R., Césari, S.N., 2008. Fossil woods in interglacial sediments from the
886 Carboniferous Hoyada Verde Formation, San Juan province, Argentina. Palaeontology
887 51, 163–171.
- 888 Purdy, D.J., Withnall, I.W., Bultitude, R.J., 2016. Geology, geochronology and geochemistry
889 of the northeast Drummond Basin Region. Qd Geol. Rec. 2016/01, 1–134.
- 890 Rasband, W.S., 1997-2016. ImageJ, U. S. National Institutes of Health, Bethesda, Maryland,
891 USA, <https://imagej.nih.gov/ij/>.
- 892 Roberts, J., Jones, P.J., Jenkins, T.B.H., 1993. Revised correlations for Carboniferous marine
893 invertebrate zones of eastern Australia. Alcheringa 17, 353–376.
- 894 Rößler, R., Philippe, M., van Konijnenburg-van Cittert, J.H.A., McLoughlin, S., Sakala, J.,
895 Zijlstra, G. & 35 others, 2014. Which name(s) should be used for *Araucaria*-like fossil
896 wood? – Results of a poll. Taxon 63, 177–184.
- 897 Sahni, B., 1932. On the genera *Clepsydropsis* and *Cladoxylon* and on a new genus
898 *Austrocleipsis*. New Phytol. 31, 270–278.
- 899 Scott, D.H., 1902. On the primary structure of certain Palaeozoic stems with the *Dadoxylon*
900 type of wood. Trans. R. Soc. Edinb. 40, 331–365.
- 901 Scott, D.H., 1924. Fossil plants of the *Calamopitys* type, from the Carboniferous rocks of
902 Scotland. Trans. R. Soc. Edinb. 53, 569–596.
- 903 Scott, D.H., Jeffrey, E.C., 1914. On fossil plants, showing structure, from the base of the
904 Waverly Shale of Kentucky. Phil. Trans. R. Soc. Lond. B 205, 315–373.
- 905 Simpson, G.A., Webb, G.E., Lang, S., 2012. Rockhampton Group (Cr). In: Murray, C.G.,
906 Blake, P.R., Crouch, S.B.S., Hayward, M.A., Robertson, A.D.C., Simpson, G.A. (Eds.),

907 Geology of the Yarrol Province central coastal Queensland. Queensland Geology 13,
908 90–110.

909 Smoot, E.L., Taylor, T.N., 1983. Filamentous microorganisms from the Carboniferous of
910 North America. Can. J. Bot. 61, 2251–2256.

911 Strullu-Derrien, C., McLoughlin, S., Philippe, M., Mørk, A., Strullu, D.G., 2012. Arthropod
912 interactions with bennettitalean roots in a Triassic permineralized peat from Hopen,
913 Svalbard Archipelago (Arctic). Palaeogeog., Palaeoclimatol., Palaeoecol. 348–349, 45–
914 58.

915 Taylor, T.N., Taylor, E.L., Krings, M. 2009. Paleobotany: The Biology and Evolution of
916 Fossil Plants. Academic Press, Amsterdam, 1230 pp.

917 Thulborn, T., Warren, A., Turner, S., Hamley, T., 1996. Early Carboniferous tetrapods in
918 Australia. Nature 381, 777–780.

919 Tidwell, W.D., Herbert, N., 1992. Species of the Cretaceous tree fern *Tempskya* from Utah.
920 Int. J. Plant Sci. 153, 513–528.

921 Veevers, J.J., Mollan, R.G., Olgers, F., Kirkegaard, A.G., 1964. The geology of the Emerald
922 1:250,000 sheet area, Queensland. Bur. Miner. Resour. Geol. Geophys. Aust. Rep. 68,
923 1–71.

924 Walkom, A.B., 1928. Fossil plants from the Upper Palaeozoic rocks of New South Wales.
925 Proc. Linn. Soc. NSW 53, 255–269.

926 Walter, M.R., Des Marais, D., Farmer, J.D., Hinman, N.W., 1996. Lithofacies and biofacies
927 of mid-Paleozoic thermal spring deposits in the Drummond Basin, Queensland,
928 Australia. PALAIOS 11, 497–518.

929 Walter, M.R., McLoughlin, S., Drinnan, A.N., Farmer, J.D., 1998. Palaeontology of Devonian
930 thermal spring deposits, Drummond Basin, Australia. Alcheringa 22, 285–314.

- 931 Walton, J., 1957. On *Protopitys* with a description of a fertile specimen *Protopitys scotica* sp.
932 nov. from the Calciferous sandstone series of Durbatonshire. Trans. R. Soc. Edinb. 63,
933 333–340.
- 934 Warren, A., Turner, S., 2004. The first stem tetrapod from the Lower Carboniferous of
935 Gondwana. *Palaeontology* 47, 151–184.
- 936 Weaver, L., McLoughlin, S., Drinnan, A.N., 1997. Fossil woods from the Upper Permian
937 Bainmedart Coal Measures, northern Prince Charles Mountains, East Antarctica. AGSO
938 J. Aust. Geol. Geophys. 16, 655–676.
- 939 Webb, G.E., 1990. Lower Carboniferous coral fauna of the Rockhampton Group, east-central
940 Queensland. *Mem. Assoc. Australas. Palaeontols* 10, 1–167.
- 941 Webb, G.E., 2000. The palaeobiogeography of Eastern Australian lower carboniferous corals.
942 *Hist. Biol.* 15, 91–119.
- 943 Webb, G.E., 2002. Latest Devonian and Early Carboniferous reefs: depressed reef building
944 after the middle Paleozoic collapse. In: Kiessling, W., Flügel, E., Golonka, J. (Eds.),
945 *Phanerozoic Reef Patterns*. Society for Sedimentary Geology 72, pp. 239–269.
- 946 White, M.E., 1964. 1963 plant fossil collections from Springsure. *Bur. Miner. Resour. Geol.*
947 *Geophys. Aust. Rec.* 1964/7, 3–17.
- 948 White, M.E., 1969. Plant fossils from the Springsure sheet area. Appendix 3. In: Mollan,
949 R.G., Dickins, J.M., Exon, N.F., Kirkegaard, A.G. *Geology of the Springsure 1:250 000*
950 *sheet area, Queensland*. *Bur. Miner. Resour. Geol. Geophys. Aust. Rep.* 123. 97–107.
- 951 White, M.E., 1986. *The Greening of Gondwana. The 400 Million Year Story of Australia's*
952 *plants*. Reed Books, Frenchs Forest, NSW, 256 pp.

954 **Figure legends**

955 **Fig. 1.** General geological map of Queensland showing the location of the Drummond and
956 Yarrol basins and the fossil wood localities.

957

958 **Fig. 2.** Detail of the geology of the Drummond Basin.

959

960 **Fig. 3.** Detail of the geology of the Yarrol Basin.

961 A. Map showing the location of the basin and the various deposits. The star indicates the
962 fossil wood locality.

963 B. More detailed map showing location of poorly exposed strata containing fossil wood
964 between the outcrops of the Lion Creek Limestone (coral faunule C) and a younger unnamed
965 limestone (coral faunule D), thus constraining the age to the latest Viséan (modified from
966 Krosch and Kay 1977 and Webb 1990).

967

968 **Fig. 4.** Camera lucida drawing of ray outlines on representative tangential sections of wood in
969 specimens DBW2 (A), DBW6 (B), and DBW5 (C) showing ray size and density in the three
970 morphotypes.

971

972 **Fig. 5.** Camera lucida drawings of two successive transverse sections of specimen DBW4
973 showing the compressed pith (P) and numerous vascular traces (arrows) departing from the
974 same level. (A) DBW4-1, (B) DBW4-2; vertical distance between the two sections is 2 mm.

975

976 **Fig. 6.** Ray height and width in the three wood morphotypes from the Drummond Basin
977 showing the absence of clearly distinct size groups. Stars: morphotype 1 (DBW2; n=47),
978 triangles: morphotype 2 (DBW6; n=49), squares: morphotype 3 (DBW5; n=50).

979

980 **Fig. 7.** General aspect of a trunk from the Yarrol Basin in cross-section showing the large
981 parenchymatous pith (P), secondary xylem (x2) and vascular traces (arrows). Drawn from
982 peel #YB2-s1.

983

984 **Fig. 8.** Camera lucida drawings of details of primary strand distribution and leaf trace
985 emission in YB1. Scale bars = 1 mm.

986 A. General view of the best preserved part of the pith-secondary xylem boundary showing
987 numerous peri-medullary primary xylem strands, two departing leaf traces (T1 and T2) and
988 the location of other traces at a different level of emission ((T)). In the zones facing T1 and
989 T2, the primary xylem contains several radially aligned protoxylem poles. The zones noted α
990 and β are interpreted to represent earlier stages of leaf trace production, β being a more
991 advanced stage than α . Slides YB1-A0 + YB1-B0.

992 B. Detail of the pair of traces (T1–T2) illustrated in A. Note the radially aligned protoxylem
993 strands facing the departing traces. Slides YB1-A0.

994

995

- 997 **Plate legends**
- 998 **Plate I. Wood morphotypes from the Drummond Basin.**
- 999 1. Morphotype I in transverse section showing two rays (R). Note a change in tracheid radial
1000 diameter (arrow). Slide DBW2-CT.
- 1001 2. Morphotype I in tangential longitudinal section with straight tracheids and relatively low
1002 rays. Slide DBW2-CL.
- 1003 3. Morphotype I in radial longitudinal section showing the araucarian pitting on the tracheid
1004 walls and araucarioid cross-field pitting (arrows). Slide DBW2-CR (focused stack).
- 1005 4. Morphotype II in transverse section showing multiseriate rays (R). Slide DBW6-CT.
- 1006 5. Morphotype II in tangential longitudinal section, with low to high multiseriate rays. Slide
1007 DBW6-CL.
- 1008 6. Morphotype II in radial longitudinal section showing the araucarian pitting on the tracheid
1009 walls. Slide DBW4-CR (focused stack).
- 1010 7. Morphotype III in transverse section with two large rays (R) and a zone of reduced tracheid
1011 radial diameter (arrow). Slide DBW8-CT.
- 1012 8. Morphotype III in tangential longitudinal section showing very broad rays. Slide DBW5-
1013 CL.
- 1014 9. Morphotype III in radial longitudinal section showing the araucarian radial pitting of the
1015 tracheids and the araucarioid cross-field pitting (arrows). Slide DBW8-CR (focused stack).
- 1016 Scale bars: 1, 2, 4, 5, 7, 8 = 100 μm ; 3, 6, 9 = 50 μm .
- 1017
- 1018 **Plate II. Primary vascular structures in specimens DBW4 (1–4) and DBW6 (5–6) from**
1019 **the Drummond Basin**

- 1020 1. View of the periphery of the pith (P) in DBW4 showing a small conspicuous departing
1021 vascular trace (arrow) with a more or less endarch maturation. A possible small strand is
1022 indicated by an arrowhead on the right. Slide DBW4-CT1.
- 1023 2. Zone of the stele in immediate continuity with that illustrated in 1, showing another
1024 vascular trace (arrow), which is located slightly further from the pith and appears to have a
1025 more mesarch maturation. A small strand at the pith periphery is indicated by an arrowhead.
1026 Slide DBW4-CT1.
- 1027 3. and 4. View of another relatively well-preserved area of the pith (P) and innermost
1028 secondary xylem (X2) showing another conspicuous vascular trace departing (arrow). The
1029 location of putative small strands of primary xylem is indicated by two arrowheads. Slide
1030 DBW4-CT1.
- 1031 5. General view of specimen DBW6 in transverse section, with a group of three small
1032 vascular traces to lateral appendages (t1–t3) visible in the wood. DBW6-CT
- 1033 6. Detail of one of the three traces in 5. DBW6-CT.
- 1034 Scale bars: 1, 2, 3, 4 = 100 μm ; 5 = 1.5 mm; 6 = 250 μm .

1035

1036 **Plate III. Primary vascular structures in specimen DBW9 from the Drummond Basin**

- 1037 1. General view of the part of the specimen with the preserved pith–secondary xylem
1038 boundary in transverse section showing the parenchymatous pith (P) with cluster of dark cells
1039 (*) and a departing vascular trace (arrow). Slide DBW9-A.
- 1040 2. View of the pith in longitudinal section showing the clusters of dark cells (*). Slide DBW9-
1041 B.
- 1042 3. Detail of a cluster in the pith showing the thickened walls of the cells. DBW9-A.

1043 4. Pith-secondary xylem boundary in transverse section, showing the apparent lack of
1044 immersed primary strands in the pith (P) and the inner wood (X2) with uni- to biseriate rays.
1045 Slide DBW9-A.

1046 5. Detail of the departing vascular trace illustrated in 1. Slide DBW9-A.

1047 Scale bars: 1 = 500 μm ; 2, 4, 5 = 250 μm ; 3 = 100 μm ;

1048

1049 **Plate IV. Trunks from the Yarrol Basin (*Ninsaria* gen. nov.): pith and primary xylem**
1050 **strands.**

1051 1. General view of the periphery of the pith (P) and inner wood (X2) in transverse section. A
1052 departing leaf trace (T) is visible on the right. Slide YB1-E0.

1053 2. Detail of pith cells with a dark content. Slide YB1-E0.

1054 3. General view of the periphery of the pith in transverse section showing four very small
1055 peri-medullary primary xylem strands composed of a few tracheids (yellow arrowheads).
1056 Note enlarged rays in the innermost secondary xylem (X2). This region corresponds to the
1057 zone between the traces T1 and T2 on Fig. 8. Slide YB1-A0.

1058 4. Detail of the small peri-medullary primary xylem strand indicated by an asterisk on the
1059 previous view. Note the endarch maturation. Slide YB1-A0.

1060 5. General view of the periphery of the pith in transverse section showing part of a departing
1061 leaf trace (T) and three peri-medullary strands (arrowheads), two small (left arrowheads) and
1062 a larger one (right arrowhead). Note the considerable difference in size between the strands
1063 and the trace. Slide YB1-E2.

1064 6. Detail of the large peri-medullary primary xylem strand indicated by an asterisk on the
1065 previous view. Slide YB1-E2.

1066 Scale bars: 1 = 2 mm; 2 = 50 μm ; 3, 5 = 500 μm ; 4, 6 = 100 μm .

1067

1068 **Plate V. Trunks from the Yarrol Basin (*Ninsaria* gen. nov.): leaf trace production.**

1069 1. Early stage of leaf trace (red arrowhead) production, with a large triangular strand
1070 transitioning closer to the pith-secondary xylem boundary. Secondary xylem files are starting
1071 to curve. A small strand composed of a few tracheids is visible on one side of the future trace
1072 (yellow arrowhead). Peel YB2-s1.

1073 2 and 3. Two examples of a more advanced stage of leaf trace production showing the
1074 production of additional protoxylem strands in a radial plane (red arrowheads). Two small
1075 strands composed of a few tracheids are present, one on each side of the future trace (yellow
1076 arrowheads). 2: Slide YB1-A0, corresponding to trace T2 on fig. 8; 3: Slide YB1-E0.

1077 4. Later stage of leaf departure showing the large departing trace with radially aligned
1078 protoxylem strands. Slide YB1-E1.

1079 5–7: details of the primary xylem strands seen in 2, 3, and 4.

1080 Scale bars: 1, 2, 3, 4 = 500 μm ; 5, 6, 7 = 100 μm .

1081

1082 **Plate VI. Trunks from the Yarrol Basin (*Ninsaria* gen. nov.): secondary xylem.**

1083 1. Innermost wood showing enlarged rays at the contact with the pith (P). Slide YB1-E2

1084 2. Typical wood in transverse section showing multiseriate rays (R). Slide YB1-E2.

1085 3. Detail of a zone showing variations in tracheid shape, size, and wall thickness. Slide YB1-
1086 E2.

1087 4. General view of the multiseriate rays in tangential section. Slide YB1-H.

1088 5. Detail of 4 showing a biseriate and two triseriate rays. Slide YB1-H.

1089 6. General view in radial longitudinal section showing rays (R) and radial pitting of the
1090 tracheids. Slide YB1-I.

1091 7. Detail of tracheid walls in radial longitudinal section showing multiseriate alternate circular
1092 pits with an oblique aperture. Slide YB1-H.

1093 8. Detail of cross-field with numerous small crowded pits. Slide YB1-H.

1094 Scale bars: 1, 2, 5, 6 = 100 μm ; 4 = 250 μm ; 7, 8 = 50 μm .

1095

1097 **Table legends**

1098

1099 **Table 1.** Ray anatomy in tangential longitudinal section for the different morphotypes of
1100 wood from the Drummond Basin. All measurements are for n = 50 rays. DBW9 is not
1101 included because only the innermost part of its wood is preserved. W: width; H: height.

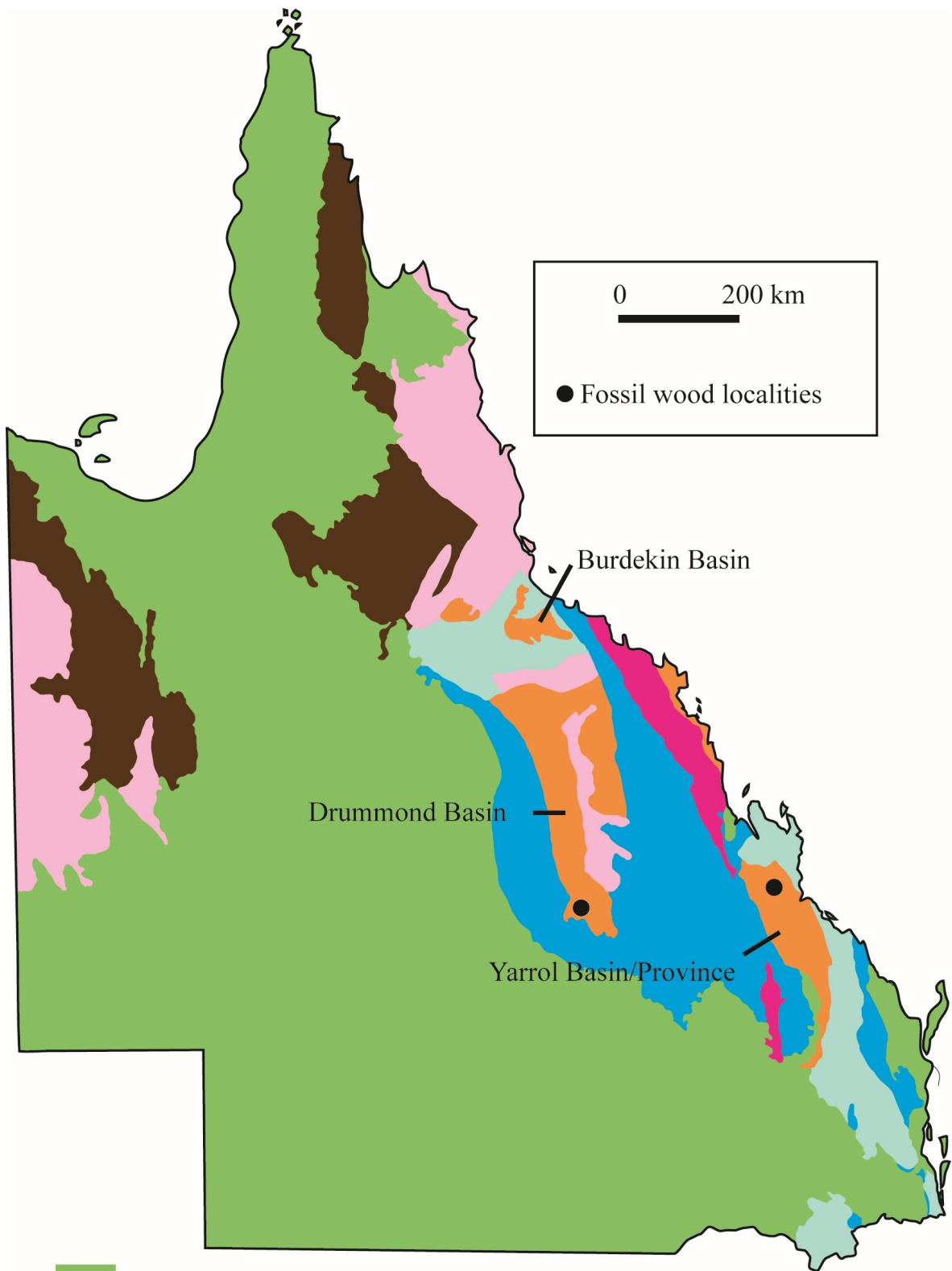
1102

1103 **Table 2.** Comparison of ray size in woods from the Ducabrook Formation and Yarrol Basin
1104 with other Mississippian arborescent taxa with multiseriate rays from Europe, North Africa,
1105 North America and Australia.

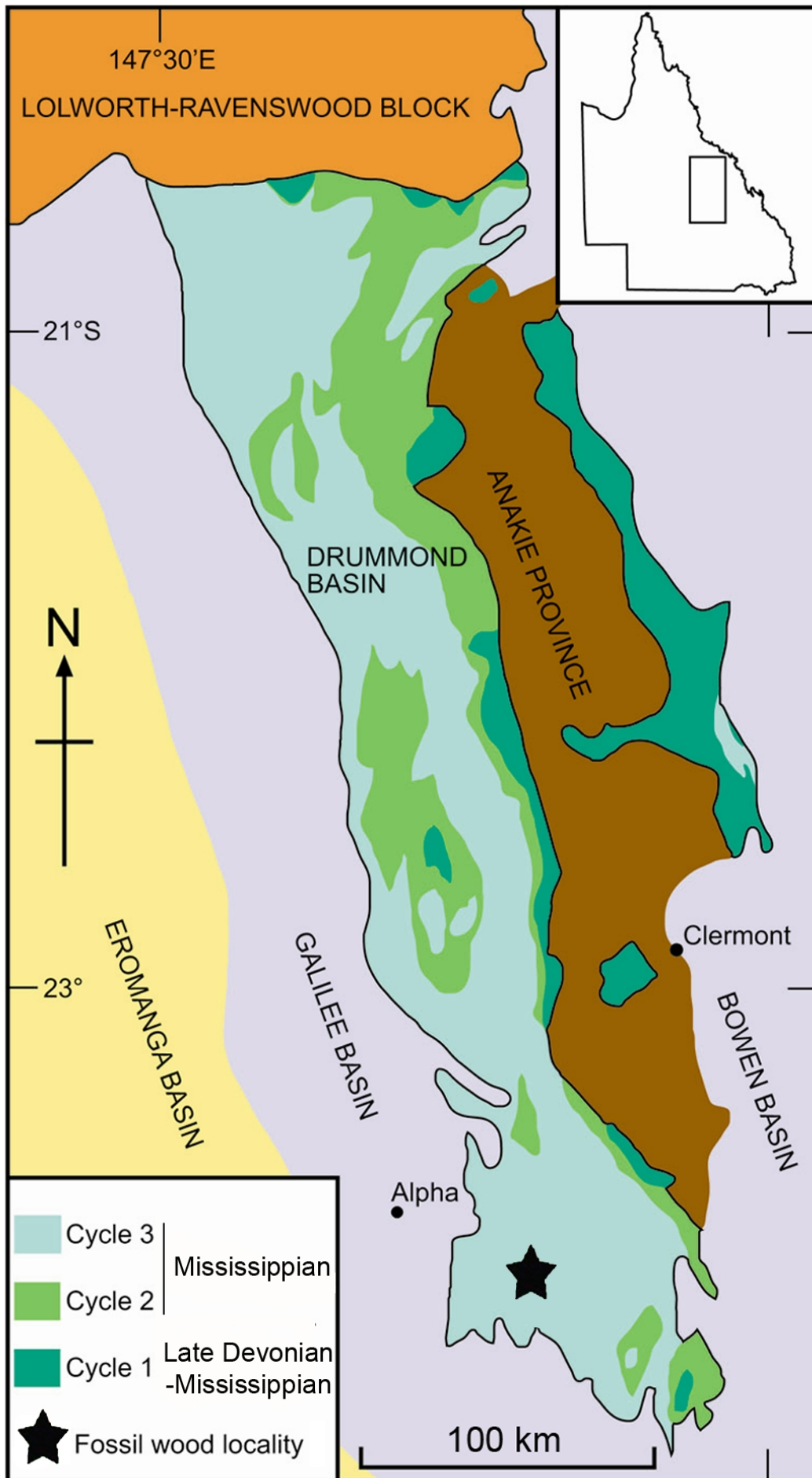
1106

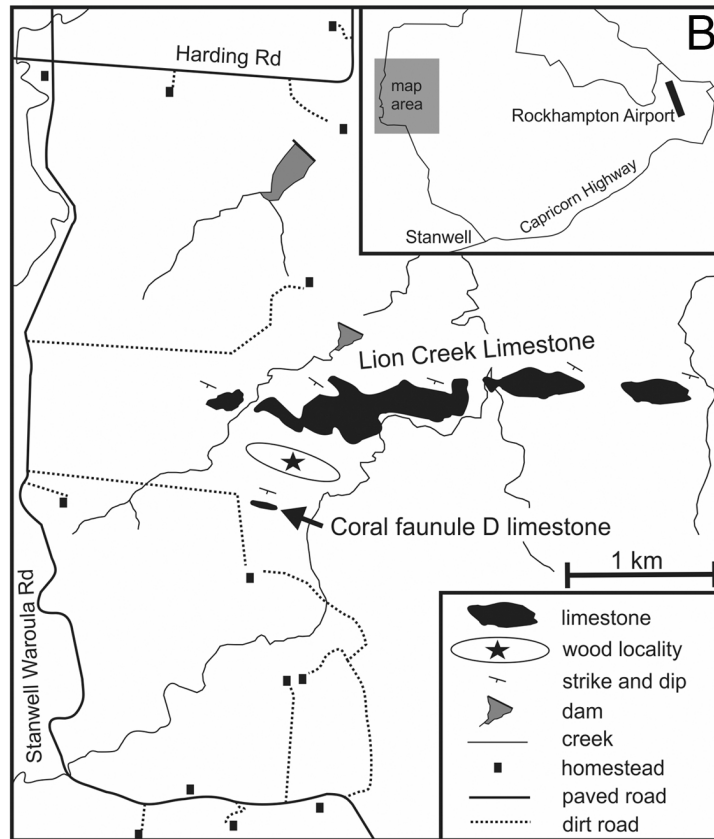
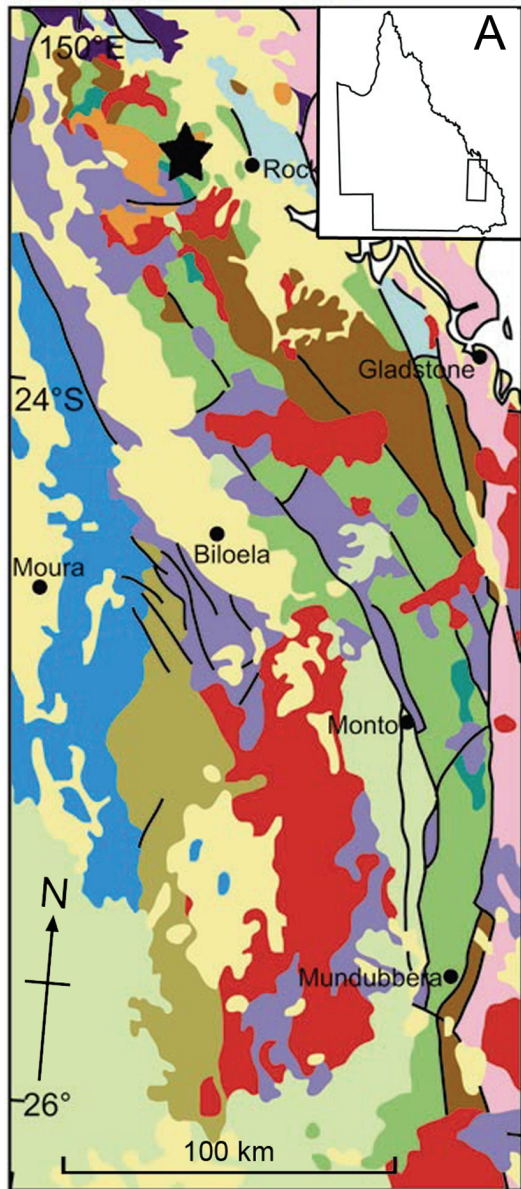
1107

1108



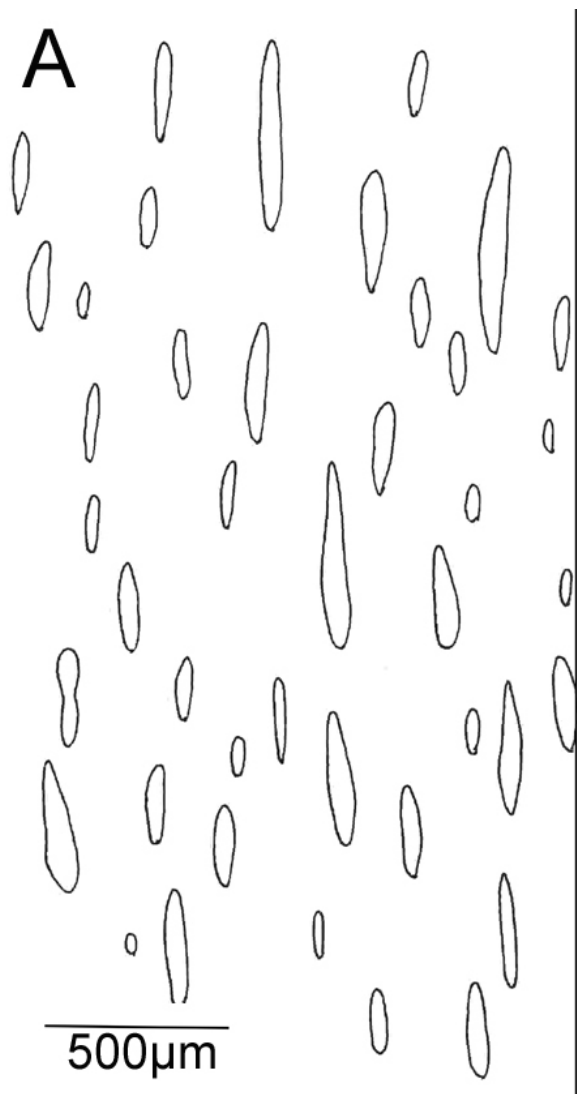
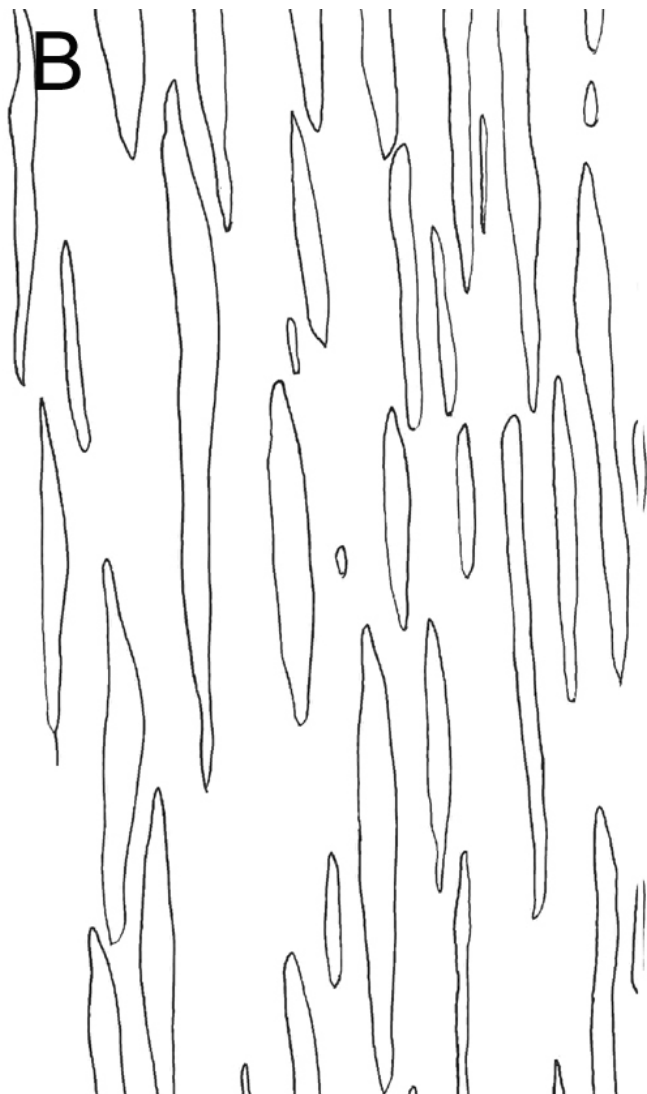
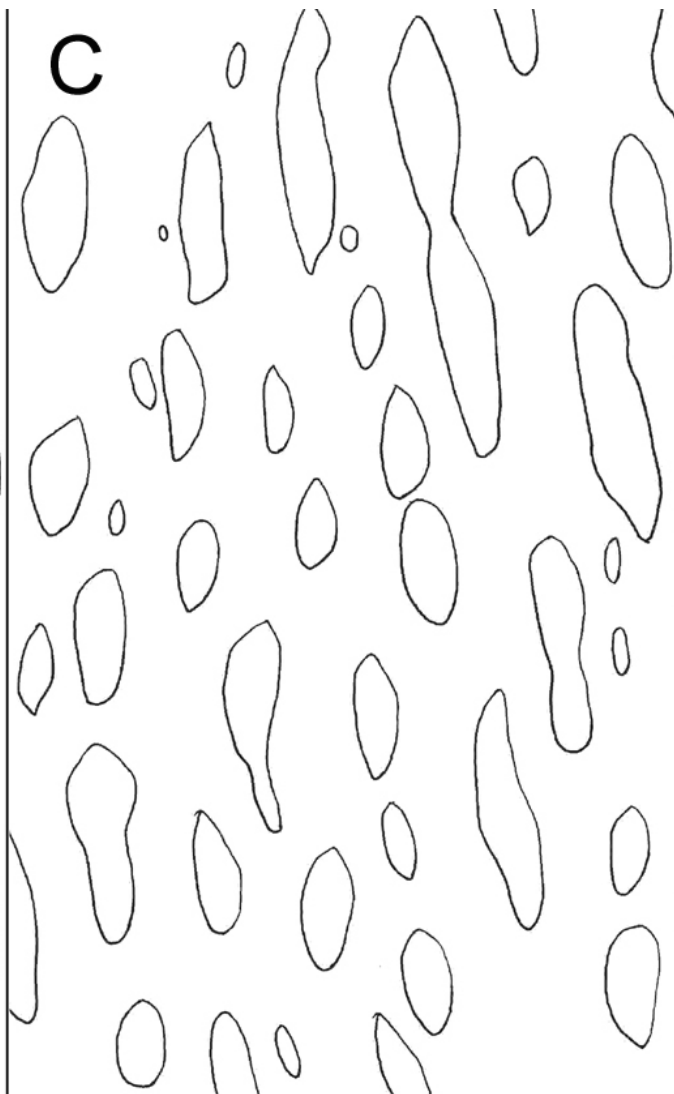
- Jurassic-Cretaceous basins
- Permian-Triassic basins
- Devonian-Carboniferous accretionary prism rocks
- Devonian-Carboniferous forearc and backarc basins
- Mid- to Late Palaeozoic arc-related rocks
- Late Proterozoic to early Palaeozoic
- Palaeoproterozoic to Mesoproterozoic rocks

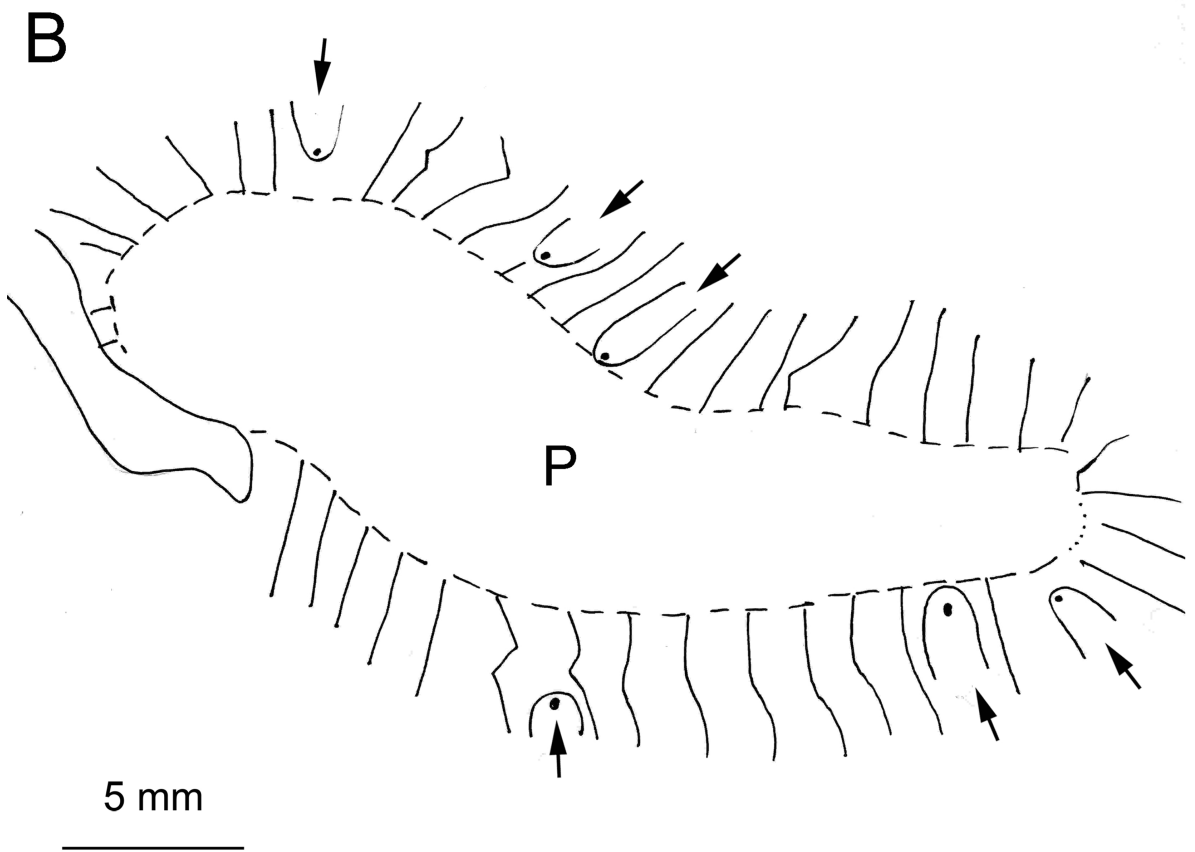
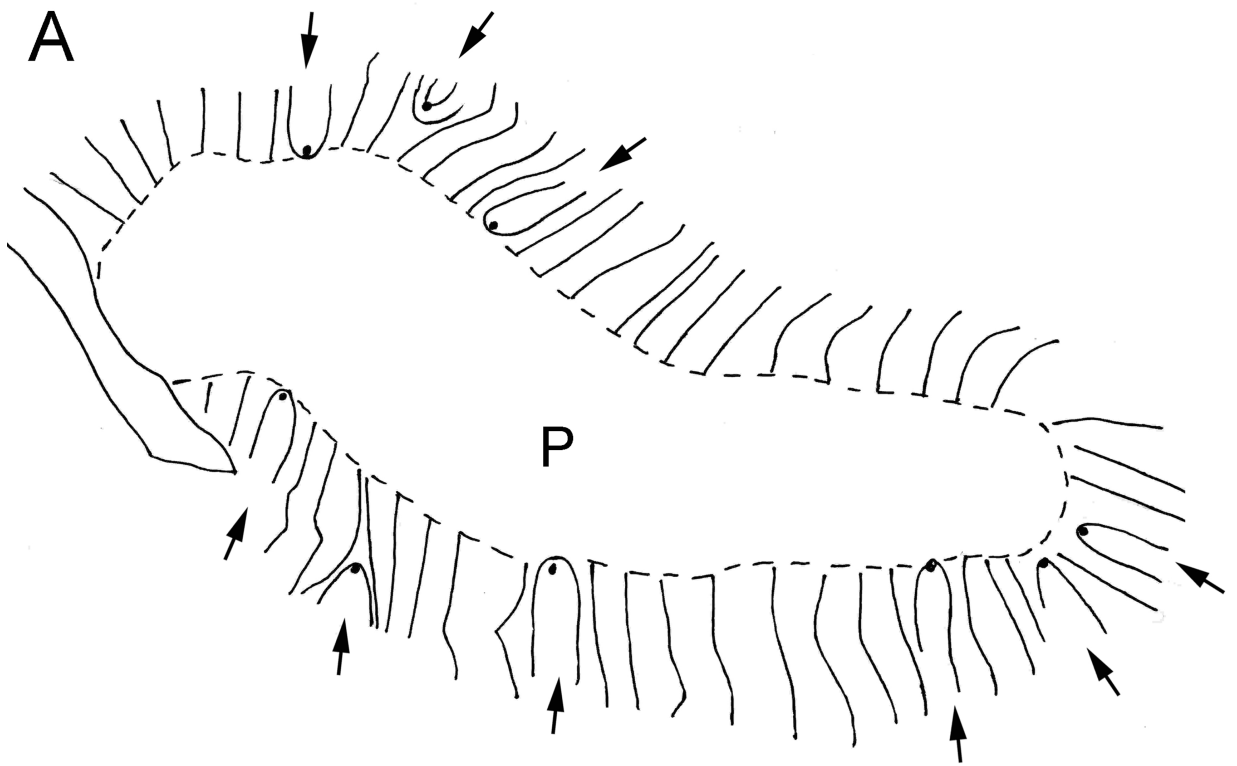




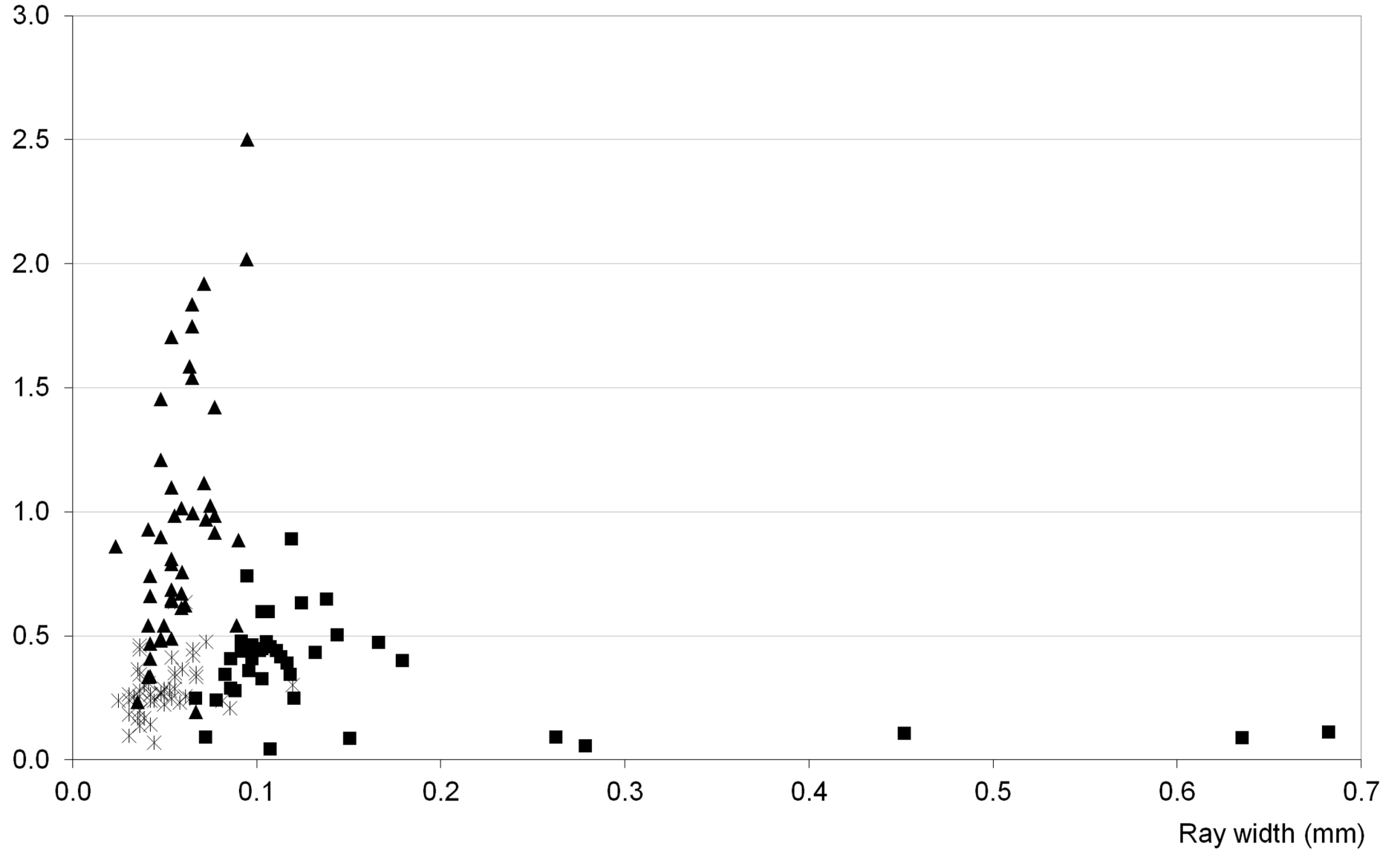
- Cenozoic sedimentary and volcanic rocks
- Cretaceous sedimentary and volcanic rocks
- Surat Basin (Jurassic sedimentary rocks)
- Permian-Triassic intrusives
- Bowen Basin (Permian sedimentary rocks)
- Gogango Ovoid Zone (Permian sedimentary rocks)
- Berzker Graben (Carboniferous-Permian sedimentary rocks)
- Connors-Auburn Block (Devonian-Carboniferous intrusives)
- Boiling Creek Group and associated units
(Late Carboniferous-earliest Permian sedimentary rocks)
- Caswell Creek & Rockhampton groups and associated units
(Late Devonian-Early Carboniferous sedimentary rocks)
- Wandilla Province
(Devonian-Carboniferous sedimentary and metamorphic rocks)
- Calliope & Philpott blocks (Devonian-Carboniferous Metamorphic rocks)
- Marlborough Block (mid-Palaeozoic metamorphic rocks)

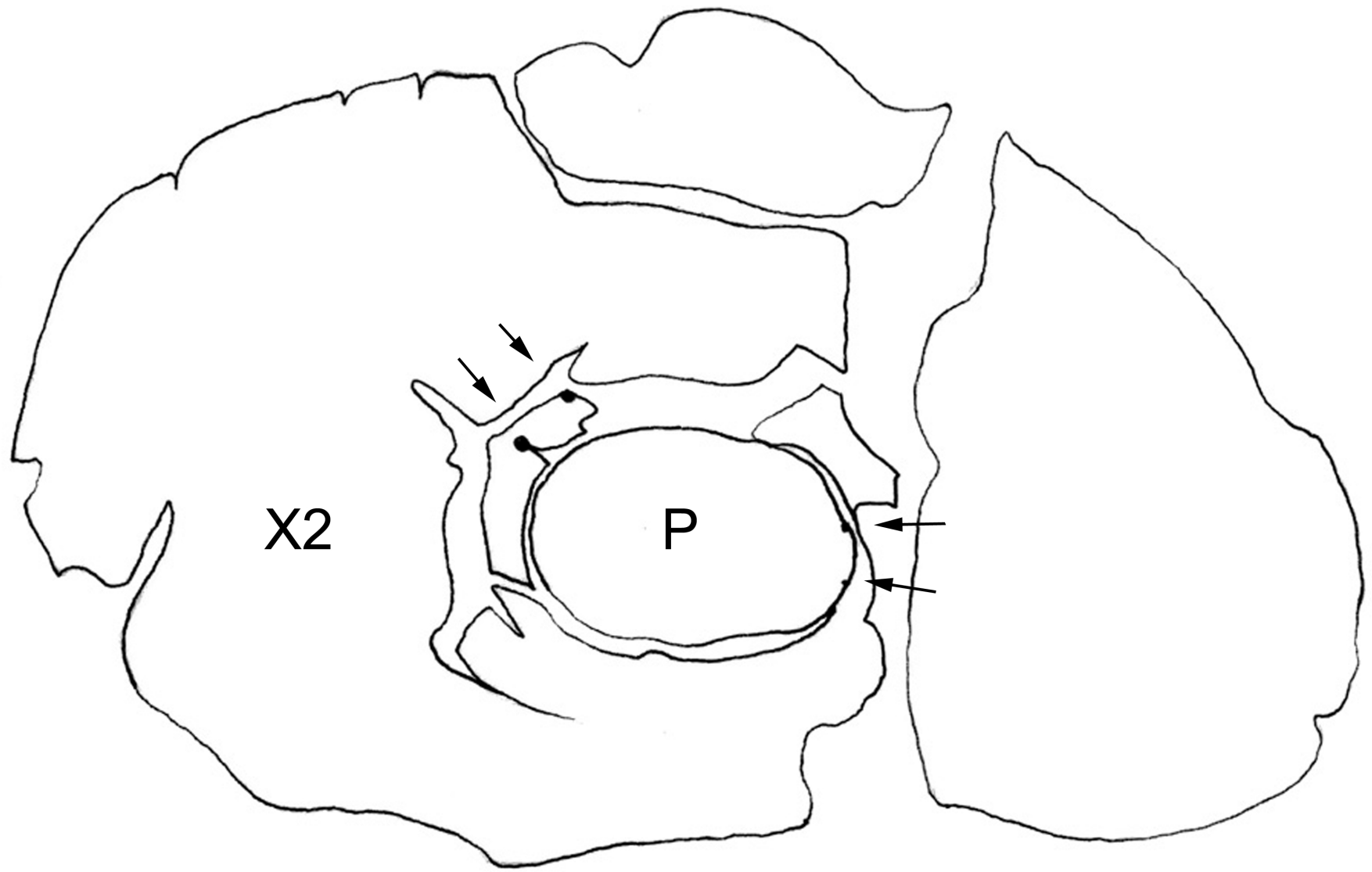
Yarrol Basin

A**B****C**



Ray height (mm)



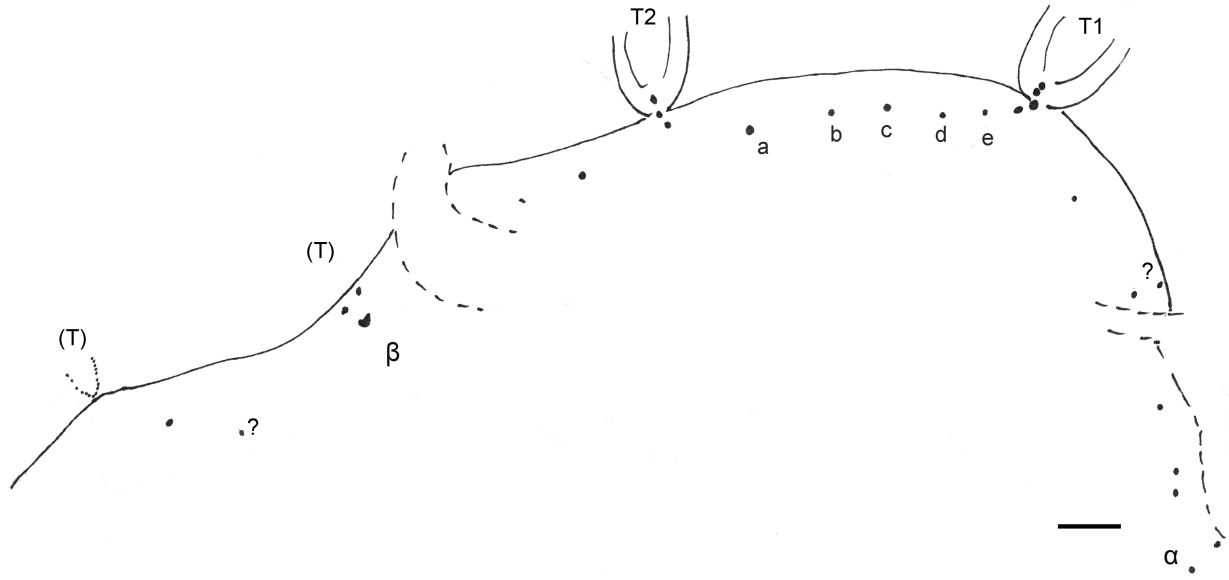


X2

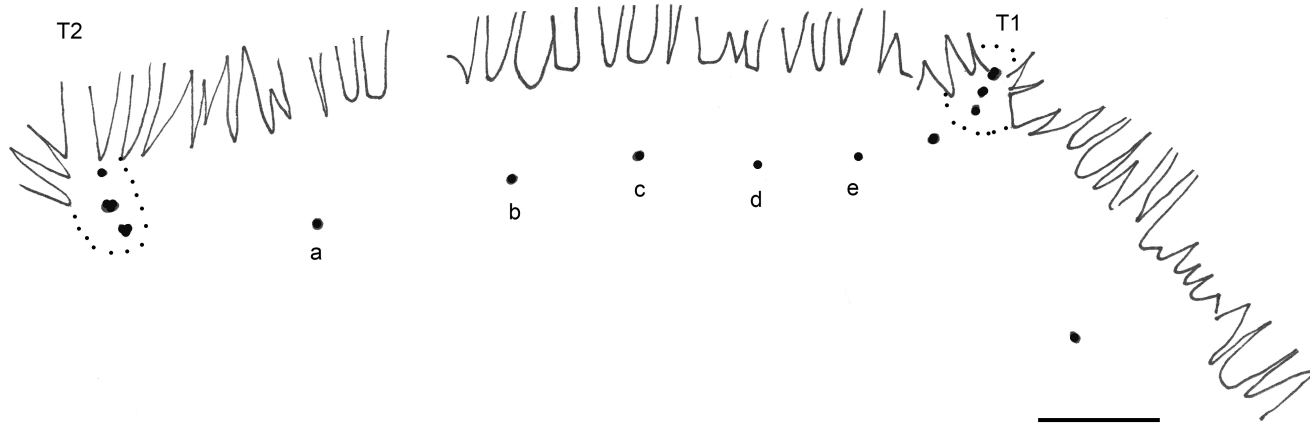
P

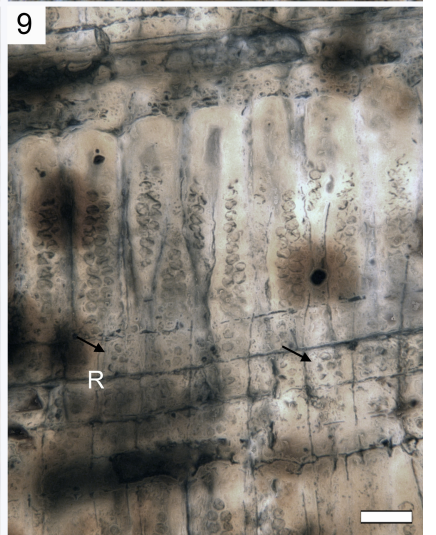
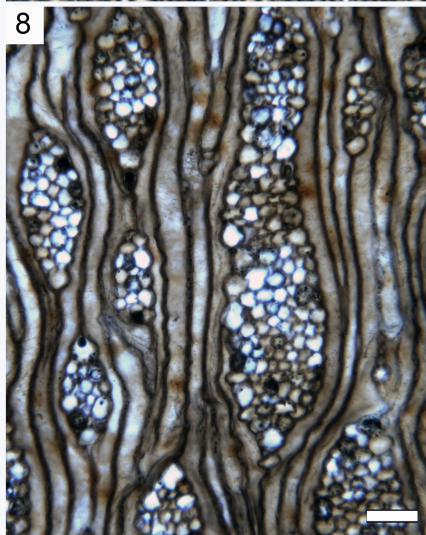
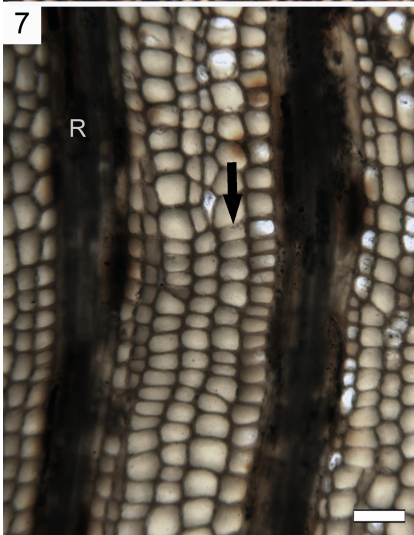
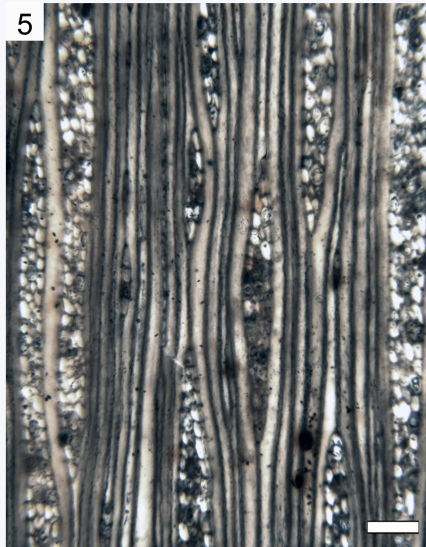
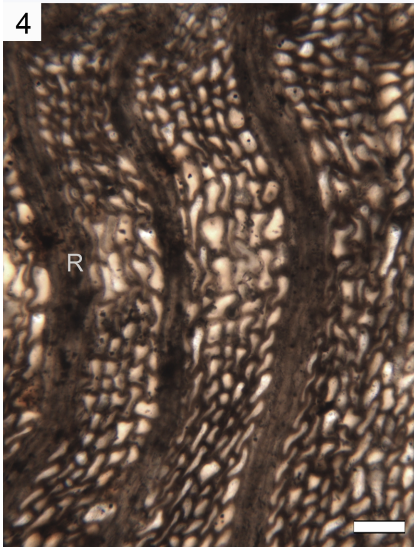
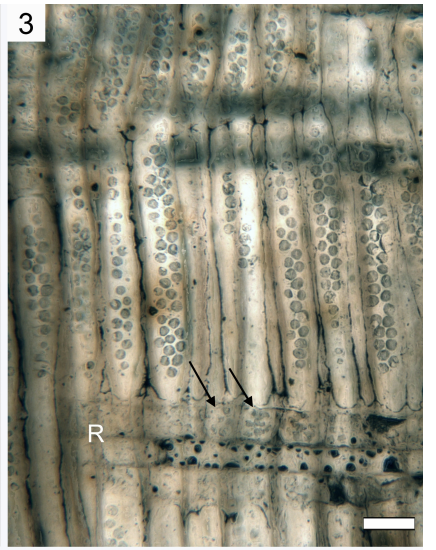
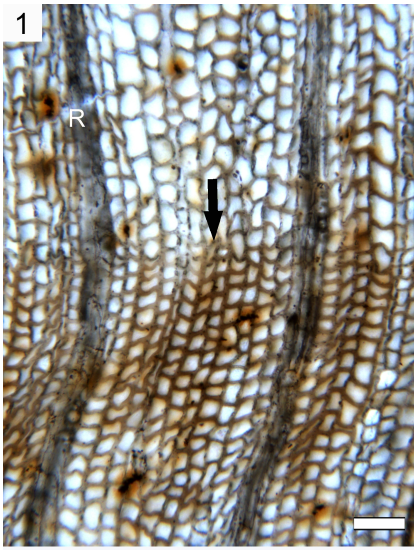
5 cm

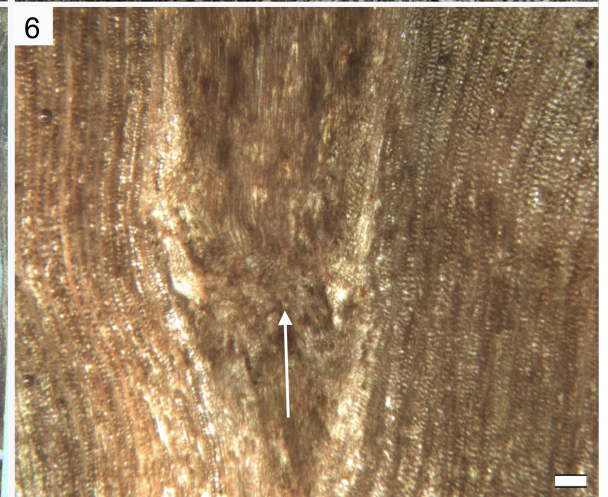
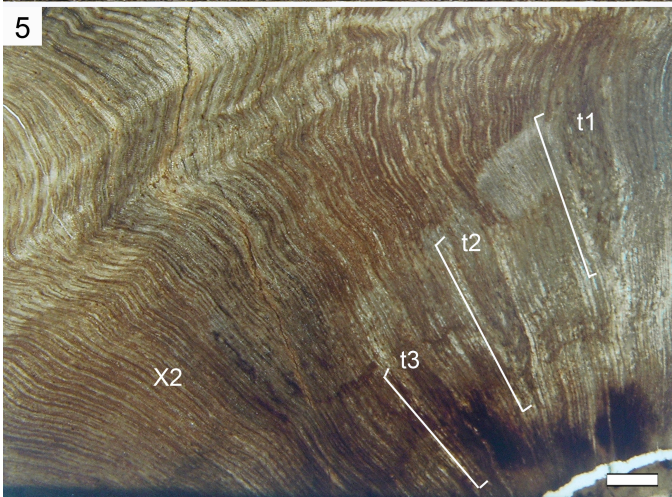
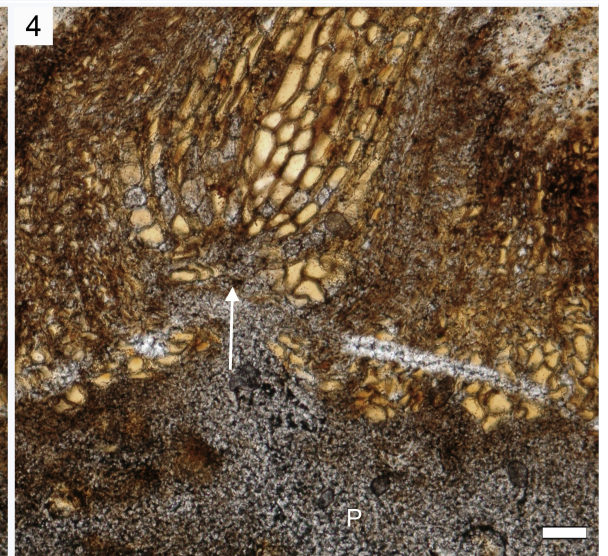
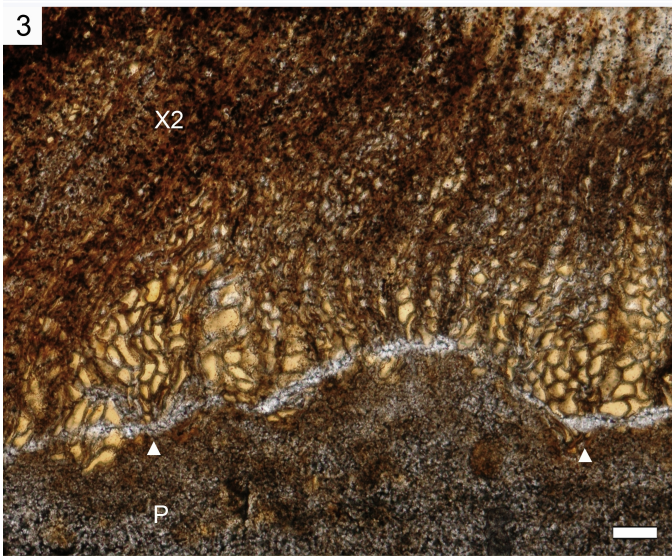
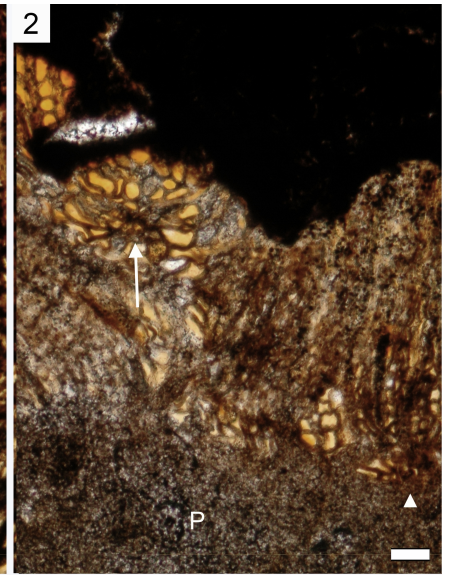
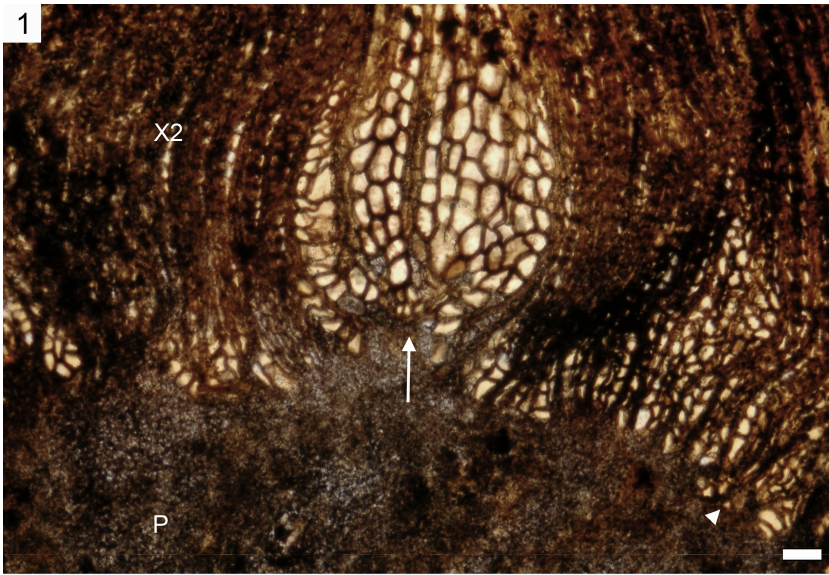
A

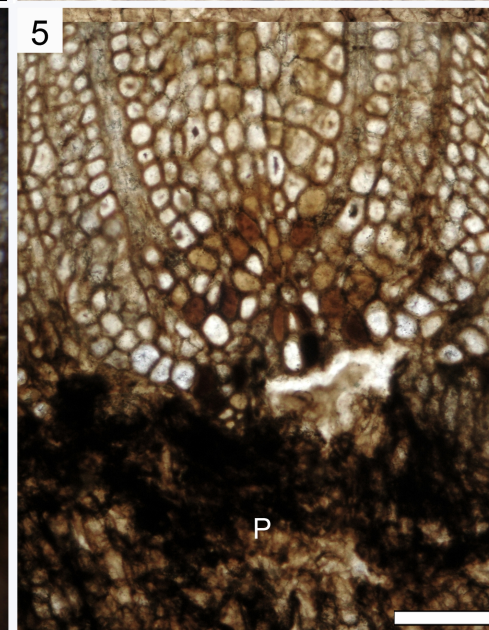
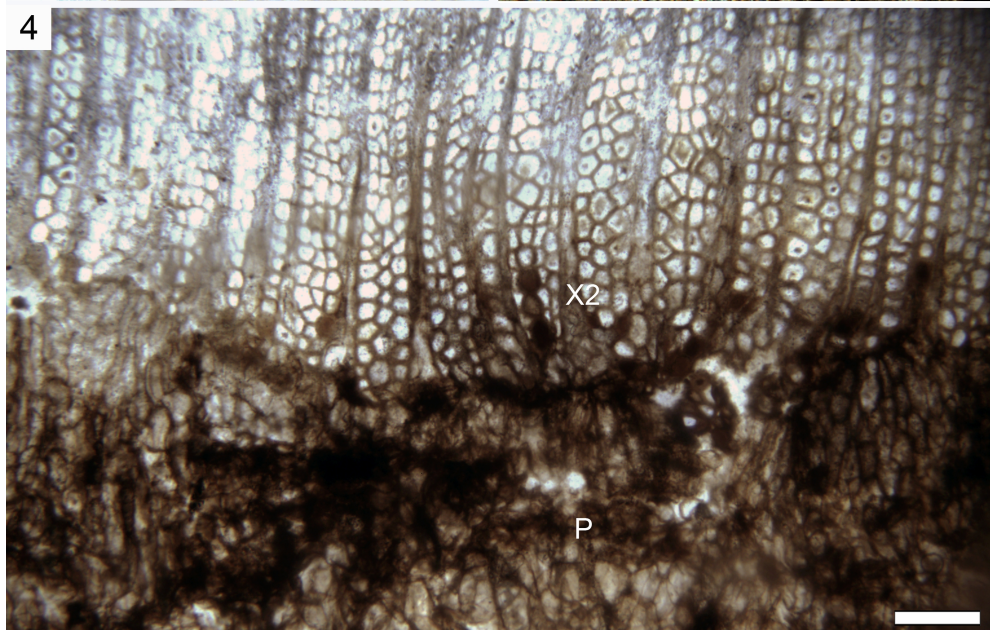
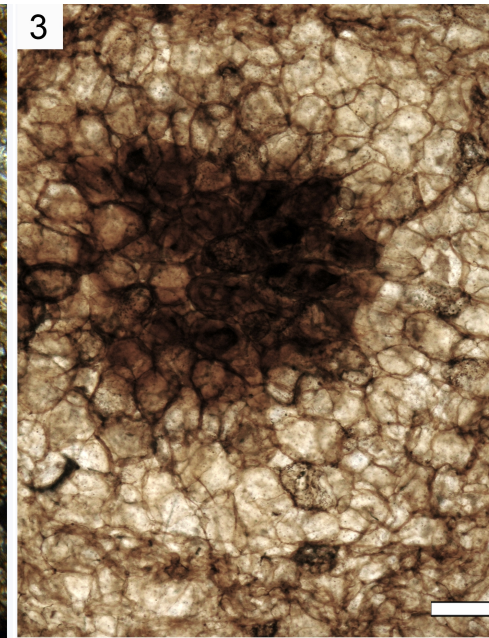
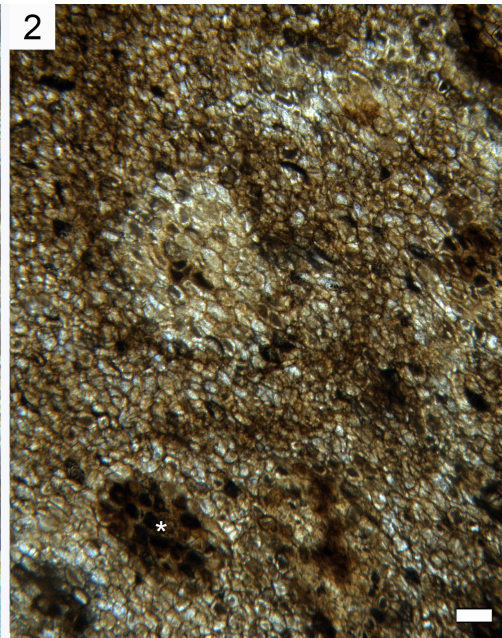
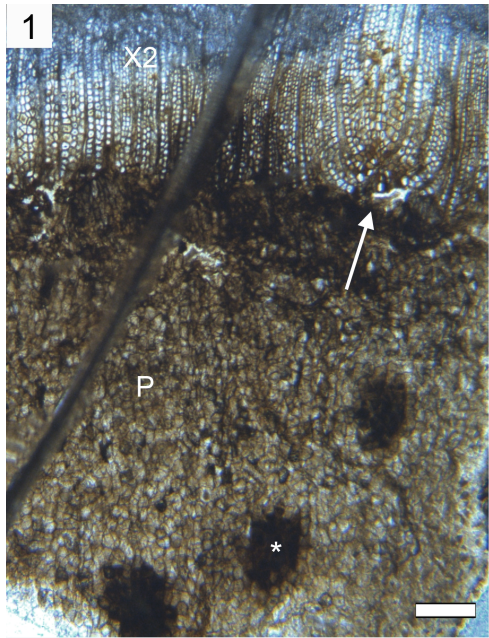


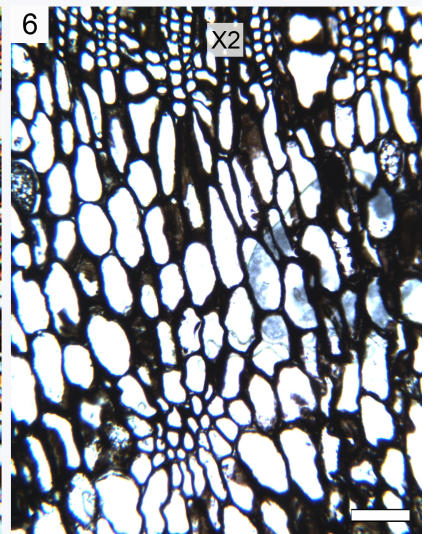
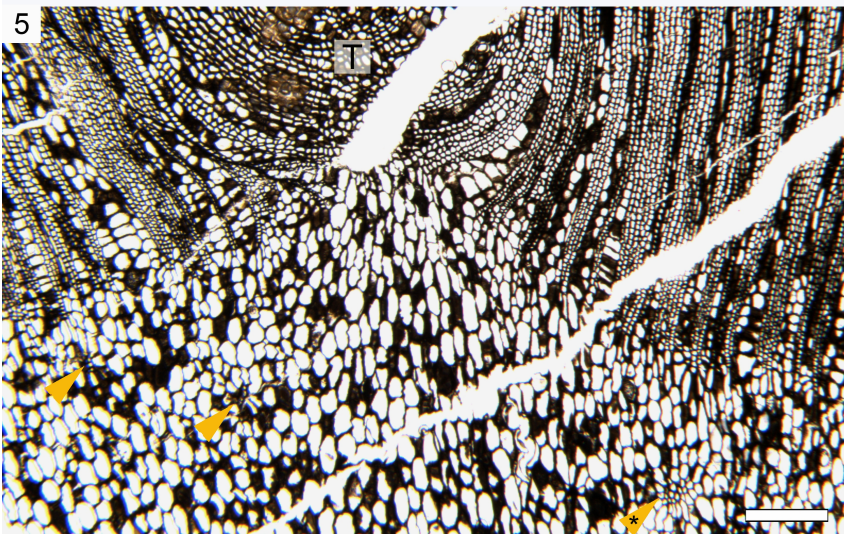
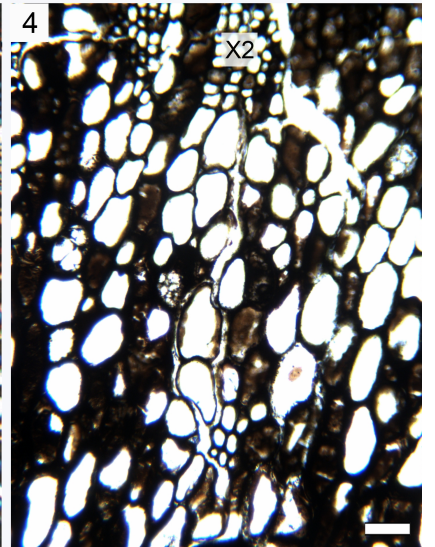
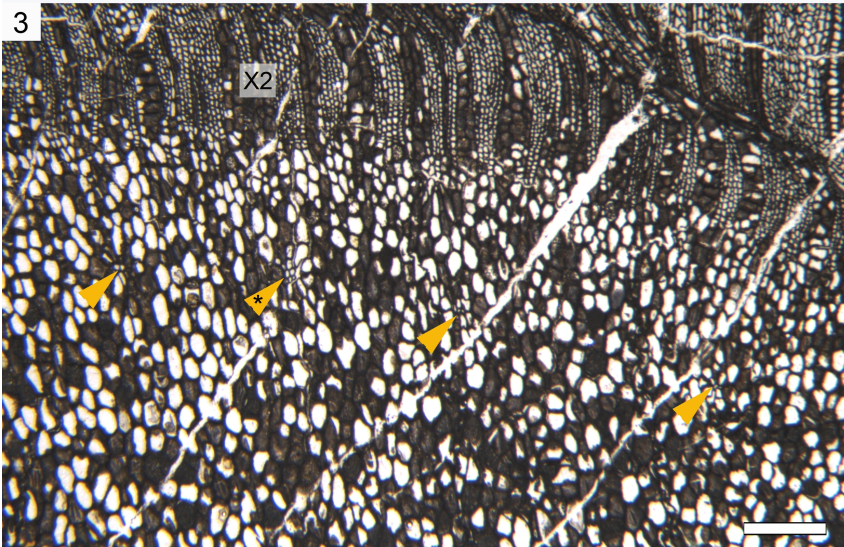
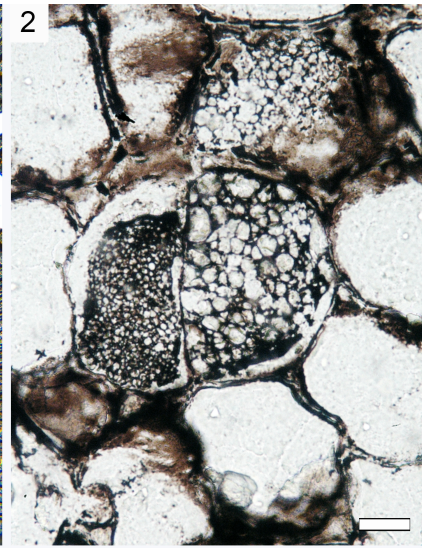
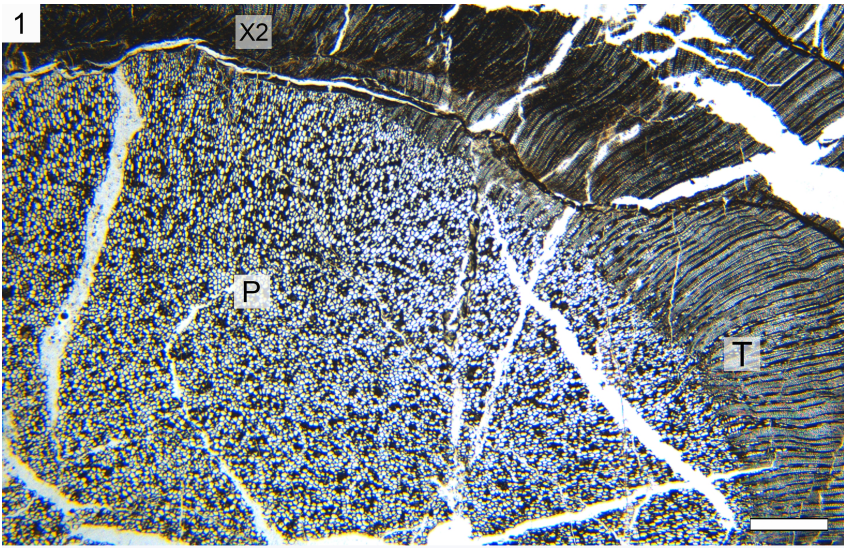
B

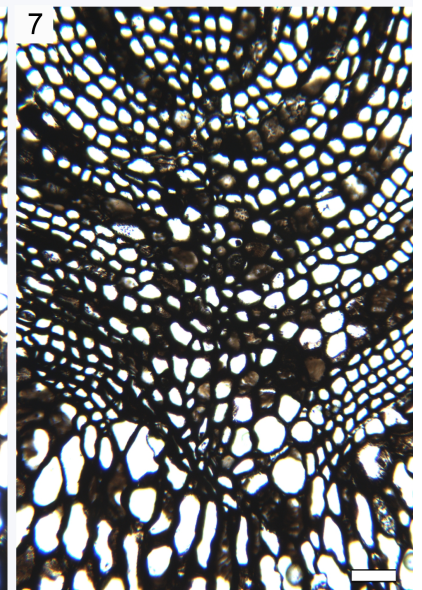
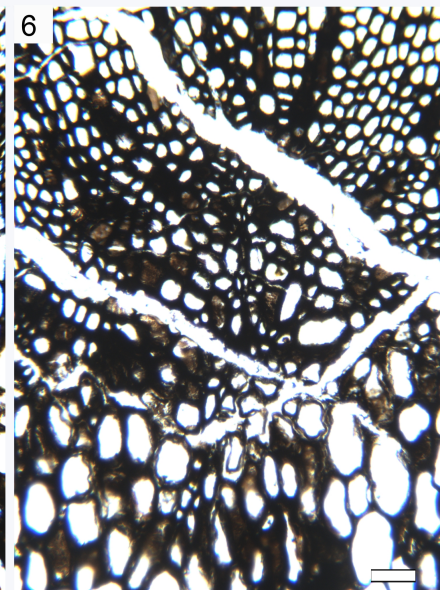
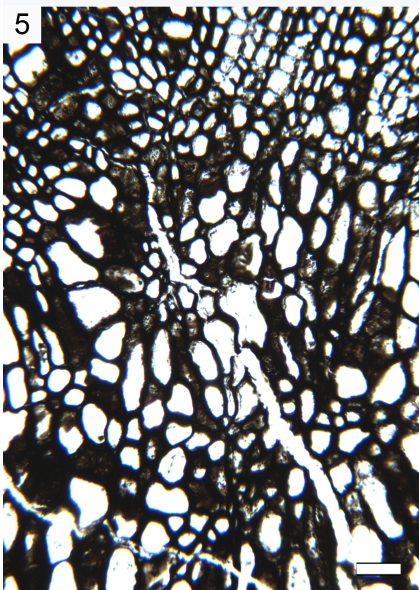
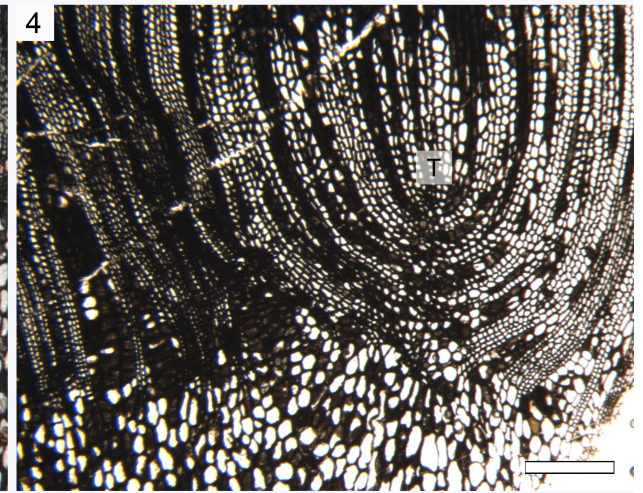
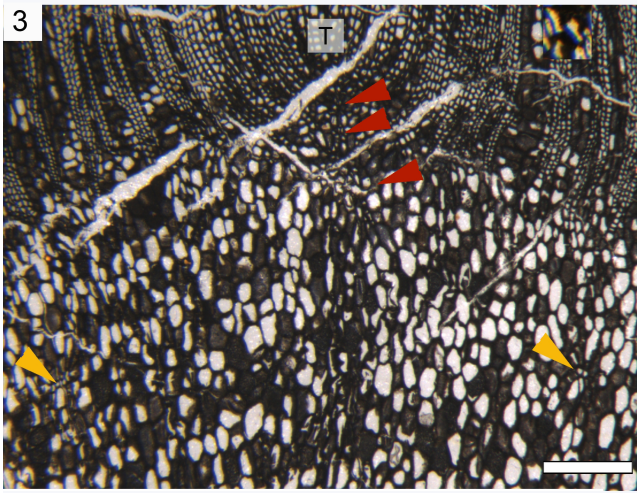
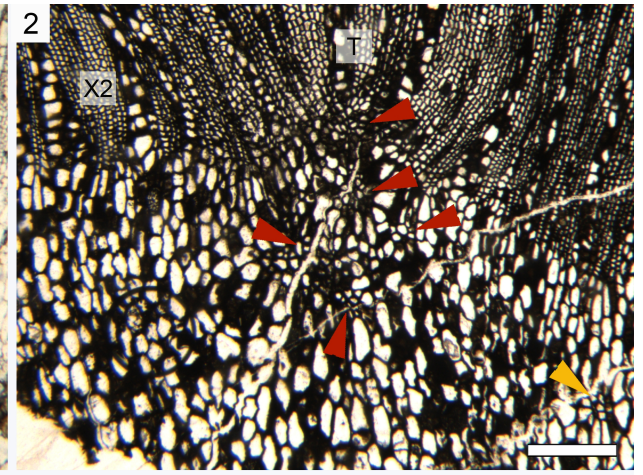
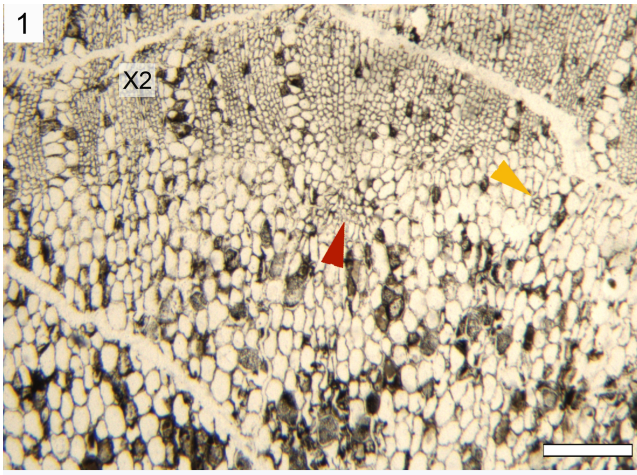


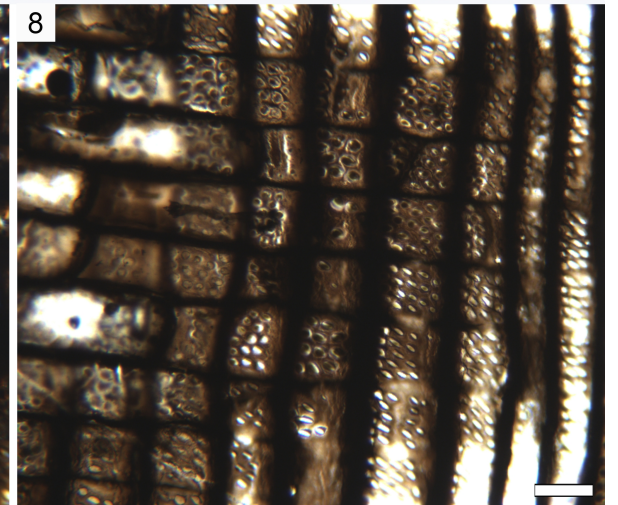
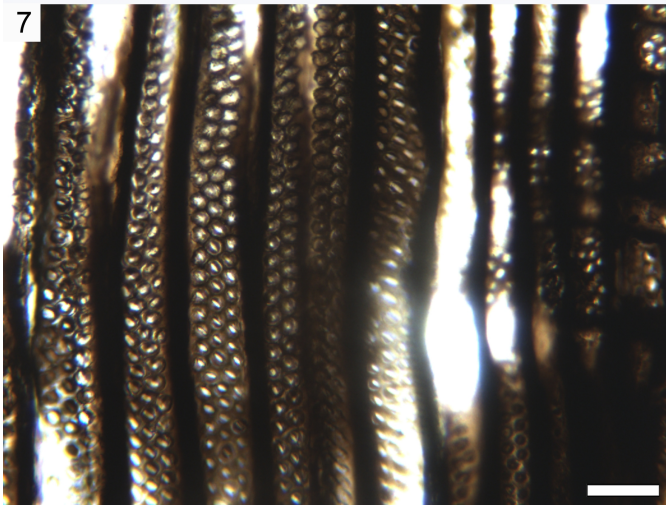
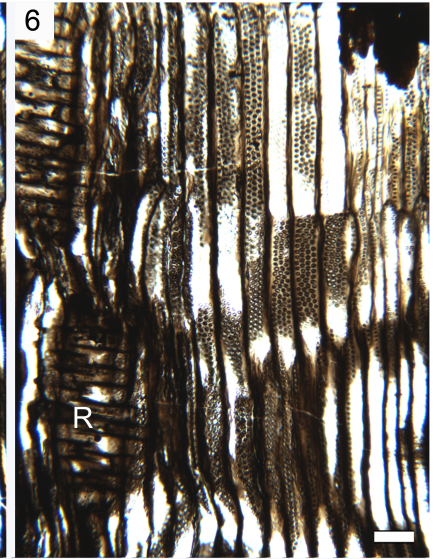
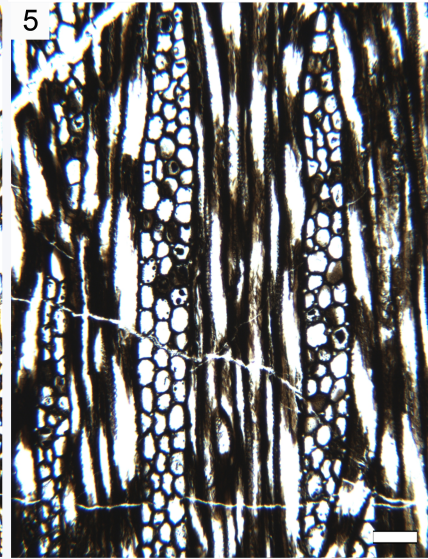
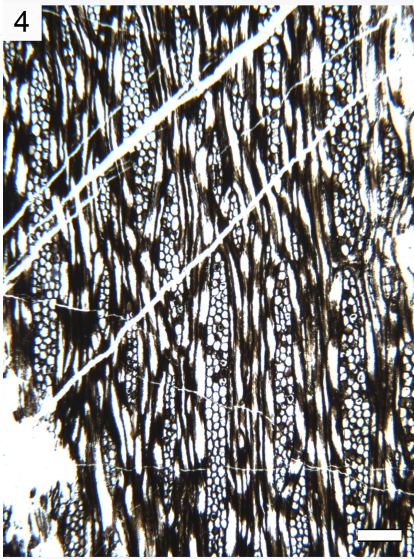
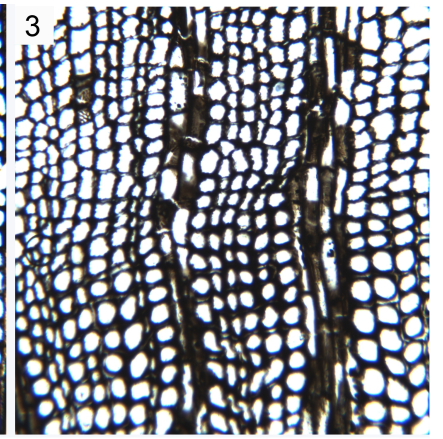
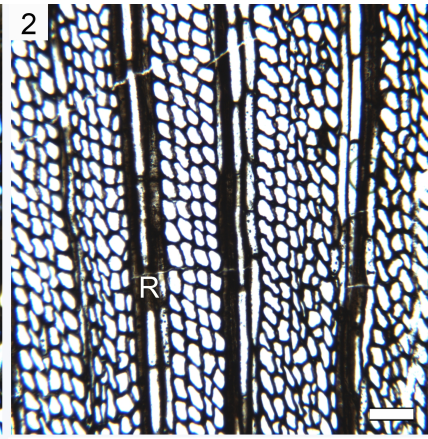
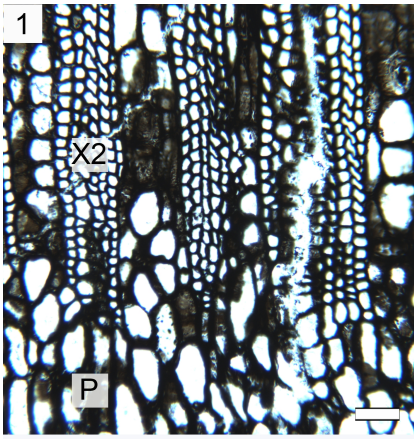












type	Ray width	Ray height	Ray cells (μm)	Ray density	Similar specimens
DBW2 Morphotype 1	Cells: 1– <u>1.8</u> –3 Max: 86 μm	Cells: 1– <u>6.2</u> –20 Max: 598 μm	W: 12– <u>22</u> –33 H: 20– <u>31</u> –57 (rectangular)	9 rays/ mm^2	—
DBW5 Morphotype 3	Cells: 1– <u>4.5</u> –8 Max: 183 μm	Cells: 1– <u>11</u> –25 Max: 1295 μm	W: 15– <u>27</u> –41 H: 19– <u>29</u> –43 (rounded)	6.5 rays/ mm^2	DBW8
DBW6 Morphotype 2	Cells: 1– <u>2.4</u> –4 Max: 116 μm	Cells: 1– <u>21.7</u> –60 Max: 2092 μm	W: 12– <u>18</u> –28 H: 14– <u>31</u> –45 (rectangular)	5 rays/ mm^2	DBW3, DBW4, DBW7, DBW10, DBW11

Table 1.

Taxon/morphotype	References	Occurrence	Width (cells)	Height (cells)
DBW2	–	Australia	1– <u>1.8</u> –3	1– <u>6.2</u> –14
DBW5	–	Australia	1– <u>4.5</u> –8	1– <u>11</u> –24
DBW6	–	Australia	1– <u>2.4</u> –4	1– <u>21.7</u> –56 (100)
Yarrol trunk	-	Australia	1– <u>2.7</u> –5	1– <u>14</u> –50
<i>Ahnetia conradii</i>	Decombeix and Galtier, 2017	North Africa	1–2 (5)	1–(<u>10–20</u>)–50
<i>Archaeopitys eastmanii</i>	Scott and Jeffrey, 1914	North America	1–6	1–many (1 mm)
<i>Cauloxylon ambiguum</i>	Cribbs, 1939	North America	1–(<u>3–4</u>)–7	1–(<u>30–50</u>)–92
<i>Dadoxylon ambiguum</i>	Frentzen, 1931 in Galtier et al., 1998.	Europe	1– <u>1.5</u> –3	1–(<u>1–10</u>)–35
<i>Eristophyton waltonii</i>	Lacey, 1953	Europe	1– <u>2</u> –5	1–(<u>5–10</u>)–50
<i>E. fasciculare</i>	Scott, 1902; Galtier and Scott, 1990, 1994.	Europe	1– <u>1.5</u> –3	1– <u>7</u> –22
<i>Faironia difasciculata</i>	Decombeix et al., 2006	Europe	1– <u>1.5</u> –4	1– <u>6.5</u> –28
<i>Megalomyelon myriodesmon</i>	Cribbs, 1940	North America	<u>1</u> –3	1–(<u>30–50</u>)–90
<i>Picnoxylon leptodesmon</i>	Cribbs, 1938	North America	<u>1</u> –3	1–(<u>10–15</u>)–50
<i>Pitus antiqua</i>	Gordon, 1935	Europe	2– <u>3</u> –5	1–70
<i>P. withamii</i>	Gordon, 1935	Europe	1– <u>1.7</u> –4	2– <u>14</u> –78
<i>P. primaeva</i>	Gordon, 1935	Europe	8– <u>10</u> –15	1–60

<i>P. dayi</i>	Gordon, 1935	Europe	4- <u>5</u> -6	1-36
<i>Pitus sussmilchii</i>	Walkom, 1928	Australia	1-4	1-24
MSM11	Decombeix et al., 2011b	Australia	1- <u>2.2</u> -6	1- <u>17.7</u> -50

Table 2.